Published in final edited form as:
Neuroimage. 2014 January 15; 85(0 1): . doi:10.1016/j.neuroimage.2013.04.113.

Neurovascular coupling in normal aging: A combined optical, ERP and fMRI study

Monica Fabiani, **Brian A. Gordon**, **Edward L. Maclin**, **Melanie A. Pearson**, **Carrie R. Brumback-Peltz**, **Kathy A. Low**, **Edward McAuley**, **Bradley P. Sutton**, **Arthur F. Kramer**, and **Gabriele Gratton**
University of Illinois at Urbana-Champaign

Abstract

Brain aging is characterized by changes in both hemodynamic and neuronal responses, which may be influenced by the cardiorespiratory fitness of the individual. To investigate the relationship between neuronal and hemodynamic changes, we studied the brain activity elicited by visual stimulation (checkerboard reversals at different frequencies) in younger adults and in older adults varying in physical fitness. Four functional brain measures were used to compare neuronal and hemodynamic responses obtained from BA17: two reflecting neuronal activity (the event-related optical signal, EROS, and the C1 response of the ERP), and two reflecting functional hemodynamic changes (functional magnetic resonance imaging, fMRI, and near-infrared spectroscopy, NIRS). The results indicated that both younger and older adults exhibited a quadratic relationship between neuronal and hemodynamic effects, with reduced increases of the hemodynamic response at high levels of neuronal activity. Although older adults showed reduced activation, similar neurovascular coupling functions were observed in the two age groups when fMRI and deoxy-hemoglobin measures were used. However, the coupling between oxy-and deoxy-hemoglobin changes decreased with age and increased with increasing fitness. These data indicate that departures from linearity in neurovascular coupling may be present when using hemodynamic measures to study neuronal function.

Keywords

Neurovascular coupling; aging; fitness; Event-related optical signal (EROS); Near-infrared spectroscopy (NIRS); Functional magnetic resonance imaging (fMRI); Event-related brain potentials (ERPs)

Introduction

The most commonly used methods for functional neuroimaging, such as functional Magnetic Resonance Imaging (fMRI) and in particular the blood-oxygen-level dependent (BOLD) response, are based on imaging some of the hemodynamic consequences of neuronal activity. One area of research for which hemodynamic imaging methods have proven to be particularly useful is the study of cognitive aging – where phenomena such as

Address all correspondence to: Prof. Monica Fabiani, University of Illinois, Beckman Institute, 405 N. Mathews Ave., Urbana, IL 61801, USA, mfabiani@illinois.edu, Ph. : +1-217-244-1117, Fax : +1-217-333-2922.

increased (often bilateral) brain activation under high task-load conditions have been shown to characterize older compared to younger adults (e.g., Reuter-Lorenz et al., 2000; Cabeza, 2002; see also Schneider-Garces et al., 2009). However, a correct interpretation of these data, as well as of other hemodynamic neuroimaging data requires an understanding of the relationship between hemodynamic responses and the underlying neuronal activity across individuals and age groups.

Currently the most accepted view is that the increased blood flow measured with hemodynamic methods is correlated with post-synaptic activity (Logothetis et al., 2001), which is typically measured invasively using field potentials or electrocorticogram (ECoG), and non-invasively with electroencephalography (EEG), event-related brain potentials (ERPs), and magnetoencephalography (MEG). However, the *quantitative* relationship between neuronal activity (including post-synaptic activity) and blood flow – which we refer to here as *neurovascular coupling* – is complex (e.g., Buxton et al., 2004) and still not completely understood. One of the problems in this comparison is that the time courses of neuronal and hemodynamic measures are very different – with the latter lagging the former by several seconds. Because of its slow time course, hemodynamic activity is often considered as the summation over time of separate but partially overlapping individual hemodynamic responses, each reflecting a particular neuronal response. The way in which these responses summate is very important in determining the relationship between neuronal and vascular responses. Most methods for the analysis of fMRI data (such as GLM-based methods or fast event-related fMRI methodologies; Friston et al., 1995, 1998; Menon & Kim, 1999; Rosen et al., 1998; Dale & Buckner, 1997) are based on linear decomposition. This approach assumes that the individual responses add to each other in a linear fashion – that is, without ceiling effects, or other temporal interactions (but see Buxton et al., 2004, Lin et al., 2003, and Rosa et al., 2010, for suggestions about more complex approaches to decomposition).

Because of the importance of this assumption, a number of investigators have addressed the question of whether linear additivity of hemodynamic responses does in fact occur. A typical strategy (first employed by Fox & Raichle, 1985) has been to increment parametrically the number of stimuli presented over a relatively small interval (shorter than the duration of the hemodynamic response – effectively varying stimulation frequency) to determine whether the hemodynamic response does in fact grow linearly with stimulation frequency. This approach has suggested that the hemodynamic response increases linearly with stimulation frequency, at least in occipital areas for visual stimulation (Arthurs et al., 2000; Buckner et al, 2000; Dale & Buckner, 1997; D'Esposito et al., 1999; Huettel et al., 2001; Miezin et al. 2000; Pollman et al., 2001; Wobst et al., 2001; Wan et al., 2006; Huttunen et al., 2008), although non-linear effects have also been reported when examining activity in different brain areas or with different stimulation conditions in visual areas (Arthurs et al., 2007; Binder et al., 1994; Birn et al., 2001; Friston et al., 1998; Hewson-Stoate et al., 2005; Jones et al., 2004; Liu & Gao, 2000; Rees et al., 1997; Sloan et al., 2010; Vazquez & Noll, 1998).

A problem with this approach is that it is assumed that neuronal activity would also increase linearly with stimulation frequency, even when the frequency is relatively high (e.g., greater than 0.5 Hz). For this to be true, the neuronal responses to each of the stimuli should be independent from each other. This assumption is inconsistent with data based on methods with high temporal resolution, which measure individual neuronal responses to each stimulus rather than the cumulated hemodynamic response to multiple stimuli. These data suggest the existence of strong interactions between the neuronal responses to stimuli presented at less than a couple seconds separation from each other, with these responses typically decreasing in amplitude with the number of stimulations per unit time (e.g., Adachi

Usami, 1981; Gratton et al., 2001; Van der Tweel & Verduyn Lunel, 1965; Obrig et al., 2002; Wan et al., 2006). It appears therefore that a direct comparison of neuronal and hemodynamic measures obtained concurrently (or at least in identical conditions) is required to actually test whether the two are linearly related. So far relatively few studies have in fact reported such a comparison. Typically, these studies have used electrophysiological measures (ECoG, EEG, ERPs, or MEG) to assess neuronal activity, and BOLD fMRI (e.g., Arthurs et al., 2000; Huettel et al., 2004; Wan et al., 2006) or other blood flow measures (e.g., Zaletel et al., 2005) to assess neurovascular effects. Because of the difficulty of recording electrophysiological data within a high-field MR scanner, these measures are typically obtained in separate sessions (but see Franceschini et al., 2008; Mackert et al., 2004, 2008; Huttunen et al., 2008; Ou et al., 2009, for concurrent recording of EEG or MEG data for neuronal measures and optical imaging or fMRI activity for obtaining hemodynamic data). Further, a significant problem with this approach is that the relatively low spatial resolution of some of the electrophysiological measures makes it difficult to determine whether the sources of neuronal activity are co-localized with the fMRI activation areas.

In this study we examined neurovascular coupling in primary visual cortex (BA17) using stimuli varying in frequency and a multimodal measurement approach to study neuronal and hemodynamic activity. We included ERPs and fMRI methods as gold-standard reference points, but focused on diffuse optical imaging methods as a central tool for the analysis. These methods are unique in that they allow for the concurrent measurement of both neuronal (the event-related optical signal, EROS, Gratton et al., 1995; Steinbrink et al., 2000; Wolf et al., 2002; Franceschini & Boas, 2004; Xhang et al., 2005; Tse et al., 2006; Medvedev et al., 2008; Kubota et al. 2008; Chiarelli et al., 2012; for reviews see Gratton & Fabiani, 2007; 2010) and hemodynamic activity (near-infrared spectroscopy, NIRS, Cope & Delpy, 1988; Kato et al., 1993; Villringer & Chance, 1997). Animal work (Rector et al., 1997; 2005; Foust & Rector, 2005) has shown that fast optical signals, characterized by a reduction in near-infrared light scattering, can be observed in active cortical areas[1]. A growing number of studies indicate that EROS can be used to measure mass post-synaptic activity in the brain, providing results that are consistent with electrophysiological data with respect to timing (e.g., De Soto et al., 2001; Fabiani et al., 2006; Gratton et al., 1997, 2001; Rinne et al., 1999; Tse et al., 2006; 2007; 2008; Medvedev et al., 2008; Kubota et al. 2008), and with fMRI with respect to spatial localization (e.g., Gratton et al., 1997; Gratton et al., 2000; Zhang et al., 2005). However, Steinbrink et al. (2005) reported failure to observe fast optical effects, and considered the possibility that at least some of the optical effects reported in previous papers might have reflected “non-brain” phenomena (such as generalized circulatory changes or movement artifacts). It is therefore important to eliminate the possibility that non-brain effects (such as circulatory changes and/or movements) might be responsible for the putative fast effects. In our previous work we controlled for non-brain effects by demonstrating that the signal is specific to the brain area that are supposed to be stimulated and does not extend to other areas, and by eliminating other possible confounds through experimental control. Another procedure used to control for possible spurious effects (see Medvedev et al., 2008; see also Parks et al., 2012) is to add recordings from channels with such a short source-detector distance (5–17.5 mm) to be unlikely to reach the brain. If the fast optical effects reflect brain activity, they should be visible at long (> 20 mm) but not at short source-detector distance channels; if instead they are due to non-brain phenomena they should be equally visible at both distances.

As fast optical signals are relatively novel in the study of neurovascular coupling (having only been reported by Gratton et al., 2001), to provide an additional control condition we

[1]Radhakrishnan et al. (2009) reported a failure to observe fast effects in a study using visual stimulation in two monkeys.

also recorded, concurrently with the optical imaging data, event-related potential (ERP) measures of the C1 component of the visual evoked potential, which is supposed to be generated in BA17 (Martinez et al., 1999). Specifically, we expect the latency of the peaks and response to experimental manipulations (stimulation frequency) for the C1 response to correspond to that of the EROS response in BA17.

There is also a substantial amount of evidence showing that NIRS can provide measures of hemodynamic activity that are strongly correlated with the BOLD fMRI response (see Villringer & Chance, 1997). Because the fast (EROS) and slow (NIRS) optical signals are measured using the same sources and detectors, not only can they be measured concurrently, but they can also be taken to reflect activity occurring in approximately the same segments of cortex. Although several previous studies have already used hemodynamic optical measures in the study of neurovascular coupling (e.g., Franceschini et al., 2008; Mackert et al., 2004, 2008; Ou et al., 2009), they have typically not capitalized on the possibility of measuring optical imaging to study both neuronal and vascular responses (with the exception of Gratton et al., 2001), and instead have used electrophysiological measures (ERPs or MEG) to estimate neural activity. This still leaves the problem of how to make sure that the two types of measures are taken from the same brain volume.

Simultaneous recording of neuronal and hemodynamic responses with optical imaging (using the very same optical channels to measure both) was accomplished in a previous study from our group (Gratton et al., 2001), in which we compared neuronal and hemodynamic activity in young adults in response to visual stimuli varying in frequency in a block design. The data showed that, as predicted, neuronal activity decreased with increasing stimulation frequency. Also as predicted, the hemodynamic response increased with stimulation frequency, although this effect was markedly non-linear. At first glance these data may appear to be incompatible with a linear relationship between the two. However, it should be noted that, because of the use of a block design with relatively high stimulation frequencies, the hemodynamic response should be considered as the *summation* of the responses to each individual stimulus, integrated over time. Therefore, an appropriate comparison also requires integrating the neuronal response over time, by multiplying its amplitude by the number of stimuli per unit time. When this was done the neuronal and the hemodynamic measures were found to be roughly *proportional* to each other. In other words, any increment in neuronal activity as a function of additional stimulation per unit time corresponded to a proportional increase in the hemodynamic response, providing support for a linear relationship between the two. However, the sample size (N=8) was too small to exclude that a more complex, non-linear relationship would better describe the neurovascular relationship. In the current study we used a larger sample size (n=63), and we evaluated two different models, a linear model and a quadratic model whereby the size of the hemodynamic response is proportional to the square root of the response predicted on the basis of the neuronal response integrated over time, so as to account for possible ceiling effect in the hemodynamic response as a function of increased stimulation.

An additional limitation of the Gratton et al.'s (2001) study was that the instrumentation used was based on a single light wavelength (690 nm). This did not allow for the separate computation of oxy- and deoxy-hemoglobin concentration changes (hereafter indicated by [HbO_2] and [HbR], respectively), which can only be achieved when at least two wavelengths are used. Thus, the hemodynamic measure obtained was a "composite" of changes in the concentration of the two hemoglobin species – only one of which ([HbR]) is likely to refer to the BOLD fMRI signal (Rees et al., 1997). Further, the [HbR] signal is typically much smaller than the [HbO_2] signal in most NIRS studies. In the study presented here we used a more advanced instrument capable of producing separate estimates of changes in [HbO_2] and [HbR]. In addition to the optical measures we also obtained

electrophysiological measures of neuronal activity (ERPs, measured *concurrently* with the optical measures) and BOLD fMRI data (recorded in a separate session from the same participants and with the same paradigm) to determine the extent to which the relationships observed with optical methods could be generalized to more commonly used neuroimaging techniques.

Another goal of the current research was to investigate the effects of aging on neurovascular coupling. As mentioned above, functional imaging data have been particularly important in characterizing the effects of cognitive aging within the brain (for a review, see Kramer et al., 2006). However, aging is also associated with significant changes in the cerebrovascular system. For example, cardiorespiratory fitness has been shown to attenuate the effects of aging leading to reductions in gray and white matter volumes (e.g., Colcombe et al., 2003, 2006; Erickson et al., 2011; Gordon et al., 2008) and in cognitive functions such as executive function and working memory (e.g., Emery et al., 1998; Kharti et al., 2001; Kramer et al., 1999, 2001). Research has also shown that aerobic exercise is particularly useful to delay (or perhaps even reverse) some of the effects of aging on cognitive function (Dustman et al., 1984; Colcombe & Kramer, 2003). Although the mechanisms through which these phenomena take place are not completely understood, there is substantial evidence that angiogenesis and changes in neurovasculature may play a significant role (Isaacs et al., 1992; Black et al., 1990; see also Cotman et al., 2007). It is therefore important to determine whether aging and cardiorespiratory fitness may have an effect on neurovascular coupling.

Within this context it is important to consider that, even if a linear relationship between neuronal and hemodynamic brain measures is observed for healthy young adults, departures from linearity may be observed when the cardiovascular system is deteriorating, as may be the case for low-fit older adults. A number of studies have examined the effects of aging on neurovascular coupling (e.g., D'Esposito et al., 1999; Huettel et al., 2001; Buckner et al., 2000; Niehaus et al., 2001; Rosengarten et al., 2006; Zalatel et al., 2005; for a review see D'Esposito et al., 2003), and have typically reported a diminution of the BOLD response in older adults. However, most of these studies have not involved the simultaneous measurement of neuronal and hemodynamic measures (with the exception of Zaletel et al., 2005) and none has assessed cardiorespiratory fitness in older adults. Therefore in the current study we investigated not only younger adults (as in Gratton et al., 2001), but also older adults varying in fitness levels. Because brain anatomy is known to change with aging (e.g., Kennedy et al., 2008; Raz et al., 2007) we decided to investigate neurovascular coupling within visual areas, which are reported to vary less than other areas in normal aging (e.g., Raz et al., 2005; but see Salat et al., 2004). Thus we tried to minimize the possibility of interactions between changes in neuroanatomy and functional changes in neuronal and hemodynamic responses. These data should provide a benchmark for extending this analytic approach to other brain areas and may aid the interpretation of aging data within the context of cognitive neuroscience.

Methods

Participants

Nineteen young adults (9 females, ages 20–28) and forty-four older adults (24 females, ages 65–81) participated in a five-session experiment. The older sample was larger to allow us to study the effects of physical fitness in this group (we did not expect physical fitness to play a central role in neurovascular coupling in younger adults). The oversampling of the older group also helped counteract the expected increase in variability in responses for this group. Participants were recruited using newspaper advertisements, posted flyers, and by word-of-

mouth. All participants provided informed consent in accordance with the Institutional Review Board of the University of Illinois at Urbana-Champaign.

Screening procedures and inclusion/exclusion criteria

All participants were fluent English speakers and educated in English from the primary school years. No participants reported a history of head trauma, drug abuse, visual impairment, or of neurological or psychiatric disease. None of the participants was taking beta-blockers or any drugs known to affect the central nervous system (such as neuroleptic, antidepressant, and anxiolytic agents). Only participants who scored within normal limits on the modified Mini-Mental Status exam (mMMS; Mayeux, et al., 1981), showed no evidence of depression based on the Beck's Depression Scale (BDI, Beck et al., 1996), displayed visual contrast sensitivity within normal ranges on the VCTS 6500 test (VisTech Consultants Inc., Dayton, Ohio), and scored above or within one standard deviation of the average score for their age group on the Vocabulary subtest of the Wechsler Adult Intelligence Scale - Revised (WAIS-R; Wechsler, 1981) were included in the study. Finally, older participants were required to have medical clearance from their personal physician to participate in the fitness assessment. Table 1 reports statistics for the main demographic and neuropsychological variables for the younger adults and the two older adult groups.

Biometric variables

For the older adults only, physical fitness was evaluated using the VO_{2max} index, using a modified Balke protocol (American College of Sports Medicine, 1991). The high- and low-fitness groups were selected to be within the upper and lower third of published norms, respectively. The younger adults were considered to be relatively fit when compared to the older adults, and reported moderate to high levels of physical activity.

A number of physiological measures were collected to characterize the different groups of subjects. Height, weight, and body mass index (BMI) were assessed for the older sample only. Arterial blood pressure (systolic, diastolic) and heart rate were assessed for both the younger and older samples. The mean values and *t*-statistics for each of these variables are presented in Table 2.

Sessions

The data presented in this study were collected during five sessions. The first was dedicated to the assessment of cardiorespiratory fitness (only for the older adults). The second was an MR session, for the recording of structural and functional MRI. Digitization of the locations to be used for optical recordings was performed during the third session. Both the fourth and fifth sessions were used for the simultaneous recording of optical (EROS and NIRS) and electrophysiological (ERP) data. Brain imaging data were recorded during the second, fourth and fifth sessions, while the participants were engaged in the task described below.

Task and Stimuli

During the optical/ERP recording sessions, participants sat in front of a computer monitor centered at eye-level at a distance of approximately 80 cm. The optical data were recorded over two sessions, with data from a different set of 80 overlaid optical channels (defined by a particular source-detector pair) collected from each, and their order counterbalanced across subjects. A set of 80 channels is referred to as a "montage."

A session consisted of 60 blocks, each lasting 60 seconds. Each block started with 20 s of fixation (a fixation cross was presented at the center of the screen), followed by a stimulation period lasting 19.2 seconds, and then followed by a 20.8 seconds fixation-only

period. During the stimulation period, a black and white checkerboard appeared and the cells reversed color (i.e., black to white and vice-versa), with a frequency that varied in different blocks. Each reversal was considered as a stimulus. The total amount of light generated by the computer screen was identical during all phases of the stimulation, and did not vary when a reversal occurred, as the color reversal of each square leads to an isoluminant condition. The participants' task was to fixate at the center of the checkerboard. Brief rest periods were given every 5 blocks.

The checkerboard subtended a visual angle of 15 degrees horizontally and 17 degrees vertically, and had a spatial frequency of 0.4 cycles/degree both vertically and horizontally. The reversal frequencies used were 1.0417 Hz (1-Hz condition), 2.0833 Hz (2-Hz condition), 4.1667 Hz (4-Hz condition), 6.25 Hz (6-Hz condition), and 8.3333 (8-Hz condition). These stimulation frequencies (apart from 8.33 Hz) are factors of the optical recording sampling rate (62.5 Hz), allowing for an integer number of sampling points to occur between stimuli. The reversal frequency conditions were presented with the following order (twice for each montage): 1-Hz, 2-Hz, 4-Hz, 6-Hz, 8-Hz, 1-Hz, 2-Hz, 4-Hz, 2-Hz, 1-Hz, 8-Hz, 6- Hz, 4-Hz, 2-Hz, 1-Hz. Unequal numbers of blocks were used for the different reversal frequencies to reduce the variability in the number of reversals (stimulations) across conditions, by increasing the number of blocks at the lowest frequencies.

The stimulation conditions during the fMRI session were identical with respect to stimulation timing. However, only one repetition of the 15-block order cycle described above was used and stimuli were presented using LED goggles. Within the limitations of the goggle system, the visual angles and spatial frequencies were as close as possible to those used in the optical/ERP sessions.

Structural MRI

All subjects included in this study underwent a high-resolution structural MRI scan in a Siemens 3-Tesla Magnetom Allegra MR Headscanner. Using an MPRAGE sequence, a 144-slice scan with a 1.2 mm slice thickness was obtained either in the sagittal or axial plane. The pulse parameters used in the MR recording included a repetition time of 800 ms, an echo time of 4.38 ms, and a flip angle of 8°. The field of view was 240 x 240 x 172.8 mm with matrix dimensions of 192 × 256 x 144 and voxel size of 1.25 × 0.938 × 1.2mm. The structural MRI was used for co-registering the optical data onto each individual's brain anatomy (see Whalen et al., 2008).

Functional MRI

The fMRI data were collected using an echoplanar imaging (EPI) sequence, based on 16 3-mm slices, with in-plane resolution of 3.75 × 3.75 mm (64 × 64 voxels/slice), centered on the calcarine fissure. The echo time was set at 26 ms, the flip angle at 60°, and the repetition time at 2000 ms. A total of 460 scans were obtained, covering the entire period of stimulation (15 blocks of fMRI data were obtained for each subject) with an additional 20 seconds before the first block.

MRI analyses

The MRI data were analyzed using a combination of routines from the AFNI (Cox, 1996) and FSL (Smith et al., 2004) packages. AFNI was used to perform motion correction, BOLD response estimation, generating the vein masks, and Talairach transformation. FSL was used for co-registration of structural and functional images, and for generating the brain masks. In order to exclude the superior sagittal sinus a 'vein mask' was derived from the T1 scans by manually setting a threshold at the lowest level that defined the vein without including any brain tissue. The MPRAGE images were inspected manually to identify the posterior

extreme of the calcarine fissure in each hemisphere, and the point halfway between these points was used as the origin for the regions of interest (ROI). The ROI started as a sphere with a radius of 14 mm. The ROI was then masked to include only points within the FSL-defined brain region, and to exclude points in the vein mask. Any points within these ROIs that exceeded 15% change from baseline were set to 15%. Finally, the average of the percent change across the voxels in each ROI was computed. Because of recording artifacts (mostly large movements), fMRI data were only available from 48 subjects (16 younger adults, 19 high-fit, and 13 low-fit older adults).

ERP Recording

ERPs were recorded as an additional control for the EROS responses. The analysis focused on the C1 peak (a negative peak with a latency between 80 and 100 ms), which is supposed to be generated in area 17 (i.e., the ROI on which all the brain measures focused). ERPs were recorded concurrently with the optical imaging data. For this reason only a sparse montage was used, including the following recording positions (labeled according to the 10/20 system): Fz, Cz, Pz, T5, T6, P3, P4, left and right mastoid and vertical and horizontal EOG. Individual silver/silver chloride electrodes affixed with a conductive electrode paste were used for the recording. Impedance was kept below 10 kΩ. The left mastoid electrode was used as an on-line reference, but an average mastoid reference was computed offline and used for all the analyses. The data were filtered on-line using a 1–100 Hz bandpass, and digitized at 250 Hz. Because the stimulation frequency varied widely (between 1 and 8 Hz), to make different frequencies comparable with each other, the data were segmented into recording epochs of the duration of 160 ms, and an interval between −16 and 60 ms after stimulation was used as a baseline. This unusual choice was determined by the need to minimize the effect of the response to the previous stimulus during the baseline period, especially for the higher stimulation frequencies (4 Hz and greater).

ERP Analysis

Ocular artifacts were corrected using a procedure described in Gratton et al. (1983). Trials with large voltage changes (exceeding 200 μV) after eye-movement correction were discarded. The EEG responses to the first 5 stimuli for each block were also discarded, to obtain stable recording conditions. The remaining trials were averaged separately for each stimulation frequency, recording electrode, and subject. As the response varied significantly between subjects in terms of which electrode showed the largest effect, we quantified the data using the same procedure reported by Gratton et al. (2001): for each time point, stimulation frequency and subject we computed the standard deviation across electrodes, which was used as a dependent measure for all subsequent analyses. ERP data were analyzed with repeated measure ANOVAs. Corrections for lack of sphericity (correlated error terms) were performed using the Greenhouse-Geisser method (with ε values and corrected degrees of freedom reported when the conditions apply). Note that ERP data were not useable for two subjects (1 younger and one older high-fit subject).

Optical recording

Optical data were recorded using an Imagent device (ISS Inc., Champaign, IL), based on 64 laser-diode sources (32 emitting light at 690 nm and 32 emitting light at 830 nm) and 8 photomultiplier tubes (PMTs) as detectors. Only a subset of the source laser-diodes were used at one time, using the montage described in Figure 1. The light sources were 0.4 mm optic fibers, whereas 3 mm fiberoptic bundles were used for conveying exiting light to the PMTs. Source and detector fibers were held in place using modified motorcycle helmets. Hair was combed away from under the detector fibers before they were put into place; the source fibers, being much smaller, could be placed through the hair. Source fibers were paired, so that each location was illuminated by two fibers, one connected to a 690-nm laser

and the other to an 830-nm laser; the two fibers were never on at the same time. The light sources were time-multiplexed in cycles of 16 ms divided into ten 1.6-ms periods (1.6 ms "on" periods, and 14.4 ms "off" periods for each source), so that at any given time each detector could only receive light from one source closer than 6 cm distance. The amount of light transmitted between a source and a detector at distances exceeding 6 cm is negligible (Gratton & Fabiani, 2003).

The light sources were modulated in intensity at 110 MHz. The average intensity during the "on" periods was less than 10 mW per source; considering the off periods, each source emitted an average of less than 1 mW light power. Because of the low absorption and high scattering of tissue at the wavelengths used (690 and 830 nm), the resulting irradiation is several orders of magnitude below OSHA safety standards. The detector amplifiers were modulated at a frequency of 110.00625 MHz. This created a cross-correlation (or heterodyning or beating) frequency of 6.25 kHz. This frequency was used for the recording of frequency-domain data. The optical data from each detector were sampled continuously at a frequency of 50 kHz. Eight points were collected for each oscillation of the cross-correlation frequency. As each source was "on" for 1.6 ms, there were 10 oscillations per source during each multiplex period. To eliminate the possibility of cross-talk between sources, the first two cycles (.32 ms) of recording from each channel were discarded. The remaining eight oscillations (for a total of 64 digitized points) were used to compute a fast Fourier transform (FFT) yielding estimates of DC intensity (zero-frequency or average effects), AC intensity (amplitude of oscillations at the 6.25 kHz cross-correlation frequency), and phase delay for each source/detector combination (80 per montage, 160 in total) with an effective sampling period of 16 ms (62.5 Hz).

Co-registration of optical and MR anatomical data

This procedure comprised the following steps. First, the location of each source and detector was digitized in 3D with respect to three fiducial points (located on the nasion and left and right pre-auricular points) on each individual subject using a Polhemus "3Space"® 3D digitizer. Second, the structural MR obtained for each participant allowed us to co-register the source and detector positions on the MR anatomical image where the same fiducial points were marked using Beekley Spots® (Whalen et al., 2008). Third, for each participant the MR and optical source and detector points were Talairach-transformed to place them in a common space. Fourth, to further reduce the influence of anatomical variability across participants, the individual anatomical images were centered on the midpoint between the most posterior points of the left and right calcarine fissures as identified in the structural MR images. This allowed for a more accurate between-subjects co-registration of visual cortex. Fifth, surface projections of optical effects at various latencies from stimulation were obtained using a 2.5-mm grid.

EROS analysis

The optical data from each participant and channel were first corrected for phase wrapping around the 360 degrees mark, converted to 'phase change' by subtracting the mean phase, and transformed into picoseconds. Slow drifts in the phase data were then corrected using a polynomial regression method (effectively eliminating frequencies below 0.01 Hz). A pulse correction algorithm developed by Gratton and Corballis (1995) was then applied. DC and AC intensities were normalized by dividing them by the average value across each block. Following our previous work, for the analysis of EROS we employed the phase data for both 690-nm and 830-nm channels. For each channel (i.e., source-detector combination) an estimate of the standard deviation (SD) of the phase was obtained, and used to discard channels with excessive variability (SD > 220 ps), usually due to insufficient amount of light reaching the detectors to provide valid estimates. Also, channels with DC light varying by

more than 20% were not included in the analyses, as were source-detector distances smaller than 20 mm or greater than 50 mm; however channels with source-detector distances below 17.5 mm (which were expected to be minimally affected by brain activity) were analyzed separately as a control condition to verify that optical effects were in fact generated in the brain, and not in the skin or the result of movements. This procedure led to discarding approximately 20–30% of the channels, mostly because the montage comprised a large range of source-detector distances (including very short and very long ones). Although we accepted channels with SDs up to 220 ps (i.e., 7.64 degrees of phase), these channels are very rare, with the majority of the channels having SDs < 50 ps (i.e., 1.77 degrees of phase). The data were then segmented into 240 ms epochs, time-locked to each checkerboard reversal (i.e., stimulus), beginning 16 ms before each reversal. The first five stimulations from each block were discarded to generate stable stimulation conditions. The remaining epochs were used to compute average waveforms for each measurement type (DC intensity, AC intensity, and phase delay[2]). The data were then filtered to eliminate frequencies above 10 Hz, and a baseline (estimated as the average of a 32-ms peri-stimulus period) was subtracted from the data. This baseline was selected to reduce the impact of the previous trial while maintaining sufficient baseline duration. Note that this impact was less severe than for the ERP data because the greater spatial resolution of EROS results in a smaller overlap between the brain responses elicited by consecutive stimulations.

To generate surface-projected maps of functional brain activity, we took advantage of the high spatial density afforded by our recording montage by using “pi detectors” (Wolf et al., 2000), which is a way of combining data from multiple channels traversing the same voxel, in order to increase spatial specificity and decrease noise. For intensity data, a “pi detector” is obtained by multiplying the values of different channels and computing the n-root (or by computing the average of the log transforms of the intensity data). For phase data, channels are averaged (a product would not make senses since some of the values are positive and some are negative). For each participant a 2.5 mm-grid was established over the surface of the occipital scalp (centered on the mid-calcarine point, as described above). For each location of the grid, the channels whose recording volumes encompassed the location were then determined (independently for each participant). For DC intensity, AC intensity, and modulation, the logarithms of the values were averaged. For phase data, the original value (rather than the logarithm) was used because only relative values are obtained. For phase data, the different channels were then averaged together. We did not weight the channels differently depending on their intensity because this procedure would give more weight to channels with short source-detector distances, which are unlikely to probe the brain. Most points in the central grid region were within the path of several (up to 20) channels.

For each measurement type, the previous methods yielded a grid (map) of activity for each time point (15 time points; sampling rate: 16 ms), stimulation condition, and participant. These maps were spatially filtered using an 8-mm Gaussian filter (2 cm kernel), and used for statistical analysis. This analysis was conducted by computing *t*-score maps related to the difference between each value and the baseline. Each of these *t*-score maps was then converted into *Z*-score maps.

[2]Averaging phase measures is appropriate when phase variations are very small, and, as in our approach, phase wrapping is eliminated before averaging. Phase delay is a circular (periodic) variable. Therefore the average of values that are at the two sides of the wrapping point (360 degrees) is misleading. For example, the average of 359 and 1 should be 360 or 0, and not 180. However, when the variability of the phase is small (less than 30 degrees) the probability of two points of the distribution to be on opposite sides of the wrapping point is negligible, unless the mean value is already close to 360 (or 0). In our data we eliminated this last possibility by applying a phase wrapping correction *before* averaging. The combination of phase wrapping correction and elimination of channels for which large SD of the phase exceeds a relatively small criterion makes averaging phase data a safe procedure to estimate the central tendency of the phase value.

For statistical analysis and quantification we used a ROI-approach to reduce multiple comparisons (as is typically done for neuroimaging data). A ROI was established, which corresponded to the surface projection of BA17, as defined by the Talairach Daemon (http://www.talairach.org/daemon.html)[3]. Only the data within this ROI were included in the subsequent statistical analyses and quantification. First, we examined whether a significant response was obtained in area 17 at the predicted latency of activation (96 ms), when averaged across subjects and conditions, both with respect to the baseline level and with respect to the short-distance channel control condition. Following the methodology commonly used to correct for the problem of multiple comparisons, the significance of a response was estimated by comparing the *Z*-score value observed at the peak point with a criterion value estimated using the random-field theory (see Friston et al., 1995). Then, for each subject and condition we quantified the amplitude of the neural response in BA17 by averaging the time course of the EROS response for all voxels within the preset ROI, and selecting the point in the waveform with the largest response amplitude in an interval between 64 and 128 ms from stimulation. An identifiable peak (defined as a positive peak value with respect to baseline) was obtained in approximately 78% of the waveforms (245 out 315 – 5 frequency conditions for 63 subjects), and all subjects had identifiable peaks in at least two of the five conditions. These peak values were used for the comparisons across stimulation conditions and for the neurovascular coupling analysis.

Only one value per condition per subject was entered in the analyses. Thus, averaging across optode pairs and frequency and spatial filtering (which were carried out separately for each subject and condition) do not lead to correlated error terms for the statistical analyses and hypothesis testing, since the error terms and degrees of freedom were always computed across subjects (apart from the lack-of-sphericity issue described below). Data across subjects were analyzed using *t*-tests (transformed into *Z* scores) or using repeated-measures ANOVAs when appropriate, with age as a between-subject factor and frequency of stimulation as a within-subject factor. When more than one contrast was considered within the same ANOVA, corrections for lack of sphericity were performed using the Greenhouse-Geisser method (with corrected degrees of freedom and ε values reported).

NIRS analysis

The analysis of the NIRS signal was conducted in a manner similar to that used for analyzing EROS data. The major differences were as follows. First, AC intensity data were used instead of phase data. This is because the formulae used to derive the concentration of [HbO_2] and [HbR] have been developed for intensity but not for phase data (Boas et al., 2001). Second, the data were averaged across blocks (rather than across trials) separately for each subject, condition and channel, using a baseline determined by the last 10 seconds before stimulation (note that, as the data were divided by the baseline value, they hovered around 1). Third, for each grid location (within the same grid used for the analysis of EROS), the data were transformed into [HbO_2] and [HbR] changes using the formulae described by Boas and coll. (2001). As several channels with 690 and 830 nm were included for each location, the data were pooled together across channels using the “pi detector” logic described above (Wolf et al., 2000). This yielded average estimates (across blocks) of the time courses of [HbO_2] and [HbR] changes for each location, starting 10 seconds before the beginning of the stimulation period, and lasting throughout the 19.2 seconds of stimulation (checkerboard reversals), computed separately for each subject and stimulation conditions. These waveforms were down-sampled at one value every 1.60 seconds. Fourth, the average change from baseline during the period between 5 and 19.2 seconds after the onset of

[3]We also analyzed data from other ROIs (BA18 in the left and right hemispheres) but the data are not reported here for space reasons. The results are consistent with those presented here.

stimulation was used to estimate the amplitude of the response. These data were submitted to the same type of ROI analyses used for EROS.

Results

ERPs

The ERP data (see Figure 2A) revealed several peaks, including a C1, a P1 and an N1 component. Of these, only the C1 component, which has a peak latency between 80 and 100 ms, is supposed to be generated in area 17 (Martinez et al., 1999), and therefore is relevant to the current study, whereas the P1 and N1 components (although in fact larger than the C1) are presumed to be generated in extrastriate areas. The amplitude of the C1 component was quantified as the maximum standard deviation across electrodes (for each frequency) between 64 and 92 ms for the younger adults and between 84 and 112 ms for the older adults (see Gratton et al., 2001, for a similar approach). The amplitude of C1, reported in Figure 3A, varied with stimulation frequency and age. Specifically, C1 amplitude decreased as stimulation frequency increased, $F(3.32, 192.64)=22.36$, $p<.0001$, Greenhouse-Geisser $\varepsilon=0.83$. This may be due to some form of "refractoriness" of the visual system in the case in which stimuli are presented very close to each other. The C1 was also larger in the older adults than in the younger adults, $F(1, 58)=11.21$, $p<.005$. This variation in amplitude of the C1 as a function of age may reflect small but consistent anatomical variations in the shape of BA17 in different age groups, perhaps as a consequence of shrinking or displacement of the occipital cortex in the older relative to the younger adults as reported by Salat et al (2004), which may direct the dipole towards the surface in the older group.

EROS

Figure 4A shows grand average maps of the EROS response at a latency of 96 ms, collapsed across all stimulation frequencies (back view of the brain). These data are plotted so that only voxels with *Z* scores greater than 2.00 (corresponding to an uncorrected $p < .05$) are colored. These maps indicate the presence of robust and consistent responses within the BA17 ROI, which were absent when short source-detector distances were examined (middle panel).

The location of the peak of the response (Z score=4.063; critical Z corrected for multiple comparisons at $p<.05 = 2.86$) was at pixel $x=-21$, $z=-8$ (in Talairach coordinates). For the short-distance channels, the peak Z value was equal to 1.331. The subtraction map, obtained considering the difference between the maps obtained with long (20–50 mm) and short (<17.5 mm) source-detector distance channels, also showed a clear and significant peak in area 17 ($x=-21$, $z=-8$, peak Z =3.468, critical Z = 2.69).

Young and old subjects showed similar localization of the response ($x=-21$, $z=-8$ for the young subjects, and $x=-16$, $z=-11$ for the old subjects). The time course of the average EROS response *across the entire BA17 ROI* in the young and old subjects is presented in Figure 2C. This figure indicates that the peak of EROS activation in BA17 occurred at 80 ms in the young subjects and 96 ms in the old subjects, very close to the predicted values, and to the latencies of the C1 response in ERPs presented in figure 2A. Note that the BA17 responses in EROS are more evident than in the ERPs, presumably because the greater spatial resolution afforded by EROS allows for a better separation of the responses originating from different cortical regions. Additional data are also included in Figure 2 for reference purposes. First, Figure 2B includes data from the *peak voxel across subjects* in the BA17 ROI[4]. It can be noted that the peak EROS amplitude is an order of magnitude greater than the EROS values presented in Figure 2C, which are the average of all the voxels within the ROI. This is because within the ROI individual subject peaks across conditions do not

precisely overlap either in location or latency, and individual subjects' effects (presented in figure 2D using standard units) do not extend to the entire ROI. However, the average waveforms presented in Figure 2C include, for each subject, a very large number of channels (typically > 10 per voxel) and trials (on average 772 per condition), so that the error is also an order of magnitude smaller. We chose this analytic approach (average of the ROI) because we expect it to be more stable and less likely to capitalize on chance.

As mentioned, the amplitude of the EROS response was quantified as the maximum value for the average across the entire BA17 ROI in the interval between 64 and 128 ms for each subject and frequency condition. Only waveforms with an identifiable peak were used for this analysis (see Methods section). The mean values across subjects for the young and old groups are presented in Figure 3B. As for the C1 ERP component, these data show a response that decreases as a function of frequency of stimulation ($F(2.68, 163.43)=4.20$, $p<.01$; Greenhouse-Geisser $\varepsilon = .67$). A function expressing the EROS peak decrement as proportional to the logarithm of the stimulation frequency provided a good fit for the overall average ($r=-.940$), as well as for the averages of the young subjects ($r=-.982$) and of the old subjects ($r=-.885$) separately. Thus, the EROS response in BA17 resembled the C1 ERP component in terms of latency and sensitivity to experimental manipulations: the correlation between the mean values for each imaging modality (C1 ERP and BA17 EROS) was $r=0.922$ for the average of all subjects, $r=0.931$ for the young subjects and $r=0.841$ for the old subjects. However, differently from the ERP response, the EROS response was larger in the younger than in the older adults, $F(1,61)=7.12$, $p<.01$. This discrepancy probably reflects the fact that, differently from the ERP, EROS is not influenced by the orientation of dipoles with respect to the surface of the head.

NIRS

Figure 5 and Figure 6 report *Z*-score maps (across all subjects) of the change in [HbO_2] (Figure 5) and [HbR] (Figure 6) during the interval between 5 and 19.2 seconds after the beginning of the stimulation period. The data were averaged across all stimulation frequencies. In the top rows are the data for all subjects together, both for long- and short-distance channels, as well as their difference. In the middle row are separate maps for young and old subjects. In the bottom rows are average time courses for [HbO_2] and [HbR], averaged across all pixels within the BA17 ROI. The maps indicate a diffuse hemodynamic response encompassing several areas and spreading much further than the EROS response. This probably reflects the fact that different regions of the visual cortex are activated at different latencies from stimulation, and therefore are visualized together by the hemodynamic maps (which reflect slow phenomena) but not by the EROS maps (which reflect the activation at 96 ms latency only). For [HbO_2], the peak *Z* score for BA17 was 3.789 ($x= -21$, $z= 12$, critical $Z= 2.20$). No clear response was visible in the short-distance control channels. Also, the subtraction map between the long and short distance channels showed clear activation of visual areas, including all of BA17 (Z peak=3.559, x=9, z=−3, critical Z=1.97). Separate maps for the different age groups, however, revealed a clear activation in the younger adults, but no significant activation in the older adults. This latter finding was probably due to a large variability in the [HbO_2] activation patterns of the older adults, as a *t*-test on the difference between younger and older adults was not significant ($t(61)=1.22$, n.s.). This variability in the [HbO_2] activation level reflects, at least in part, variability in physical fitness: the correlation between the [HbO_2] response and VO_{2max} in older adults was significant ($r(42)=.339$, $p<.05$). These data suggest that the amplitude of the [HbO_2] response is influenced by both age and fitness level.

[4]This is still an underestimate of the peak voxel activity, as the peak voxel location within the ROI may vary between one subject and another, and we are presenting here data from the same voxel for all subjects.

We expected that neural activity would induce a reduction in [HbR], as a function of the increase in blood flow. The results presented in Figure 6 show a widespread reduction in [HbR] as a function of stimulation. The peak *Z* score for the BA17 ROI was −5.443 (*x*= 9, *z*= 12, critical Z= −2.72). Although a small effect was visible in the short-distance control condition, it did not reach significance (peak Z=−2.73, critical Z=−3.07), and the subtraction maps between long- and short-distance channel data showed a significant activation in BA17 (peak Z= −4.868, x=−3, z=7, critical Z=−2.59). There was a difference in the amplitude of the [HbR] changes in the two age groups, reflected in a significant correlation between age and [HbR] change ($r(61)=.249$, $p<.05$). However, the correlation between [HbR] change and VO_{2max} in the older adults was not significant, suggesting that the age difference was probably not due to changes in physical fitness, and generally dissociating the [HbO_2] and [HbR] responses, with one showing significant effects of age and the other showing significant effects of fitness. Interestingly, whereas in the younger adults the two responses were strongly anti-correlated ($r(17)=-.615$, $p<.005$), this correlation was not observed in the older adults ($r(42)=-.020$, n.s.). A similar variation in the coupling was observed when analyzing the correlations between [HbO_2] and [HbR] changes in individual subjects across stimulation frequency conditions (the statistical tests of these correlations were based on their Fisher transforms). The average correlations were equal to $r=-0.52$ for the young adults, and $r=-0.26$ for the older adults ($t(61)=-2.34$, $p<.05$). Thus the data indicate an age-related variability in coupling of different components of the neurovascular response (see also Safonova et al., 2004, for a similar finding). Finally, the magnitude of the [HbR] response was negatively correlated across subjects with that of the EROS response in the 1-Hz ($r=-.280$, $t(46)=-1.978$, $p<.05$), 2-Hz ($r=-.400$, $t(44)=-2.895$, $p<.005$), and 6-Hz conditions ($r=-.306$, $t(50)=-2.273$, $p<.05$, all one-directional). For [HbO_2], a significant correlation across subjects with the magnitude of the EROS response was only evident in the 2-Hz condition, $r=.318$, $t(44)=2.225$, $p<.05$. This is also consistent with the idea that, across subjects differing in age and level of fitness, the coupling between deoxy- and oxy-hemoglobin, as well as between oxy-hemoglobin and neuronal activity, are somewhat degraded.

The effects of stimulation frequency on the [HbO_2] and [HbR] responses are presented in Figure 7. The relationship between these responses and stimulation frequency was clearly not linear. The lack of linearity is not surprising, as the neuronal measures (both EROS and ERPs) showed a marked reduction of the amplitude of the response as a function of stimulation. As such, we should not expect the amplitude of the hemodynamic response (which accrues over an extended period of time) to linearly increase with the stimulation frequency. In fact, the actual increase of the hemodynamic response as a function of stimulation frequency was overall quite modest.

fMRI

The average amplitude of the BOLD response in BA17 as a function of frequency is also presented in Figure 7 (bottom panel). The BOLD response changed as a function of age ($t(46)=1.89$, $p<.05$, one-directional), with a reduced response in the older with respect to the younger adults. The difference between high- and low-fit older adults, however, was not significant ($t(30)=1.17$, n.s.).

Relationship between neuronal and hemodynamic measures

As a reminder, to evaluate the quantitative relationship between neuronal and hemodynamic measures as a function of age and fitness, we compared the way in which the two sets of measures respond to visual stimulation frequency. Hemodynamic measures relate to phenomena that accumulate over time. As a consequence, the responses elicited by each single stimulus (checkerboard reversal) should summate (note that in our paradigm,

similarly to Fox & Raichle, 1985, the number of stimulations and the stimulation frequency are perfectly correlated, since the duration of the stimulation period is constant – therefore these two labels are interchangeable). Hence, the effect of each individual stimulus on the hemodynamic response can be estimated by dividing the actual response by the stimulation frequency. If the relationship between neuronal and vascular responses is linear, these derived measures should correlate linearly with the fast measures integrated over time. An alternative model assumes that this relationship is not linear, but likely saturates at high levels of neuronal activity. In this case we might assume that a decelerating function, such as the square root of the integrated fast signal, would be a better predictor of the hemodynamic response. Since the quadratic model does not include a linear predictor, both models have the same number of free parameters, and therefore they are directly comparable to each other.

We computed the integrated fast response (EROS and ERPs) over time for each stimulation frequency condition (by multiplying the fast response by the stimulation frequency) and, for each subject separately, correlated it with the amplitude of the changes in hemodynamic measures for the same conditions. In the linear model, we used the actual values of the integrated fast response as predictors. In the quadratic model, we used the square roots of these values. Note that this model was chosen as an example of decelerated function, indicating saturation of the hemodynamic response at high levels of neural activation. A logarithmic or exponential model would likely produce very similar results, but these models cannot be effectively separated from the quadratic model tested here with the small number of available points per subject. As we assume that the absence of stimulation would not generate a response, we added an additional point to the computation of the correlation coefficients in which both the neuronal and the hemodynamic responses are equal to 0. For all statistical analyses of the correlation coefficients across subjects we used their Fisher transforms. The average Fisher-transformed data were then reversed to correlation coefficients for display purposes.

Scatter plots between the average predicted values according to the linear and quadratic models and the various neurovascular effects for each stimulation frequency condition are shown in Figure 8. The correlations between the *predicted* and *actual* neurovascular responses for both the linear and the quadratic models, computed separately for each subject and then averaged across subjects, are presented in Figure 9. When EROS was used to estimate the neuronal response, for the three hemodynamic measures correlations were significantly different from 0 (all $|t|$'s$(61) > 3.995$, $p < .0002$). However, the quadratic model yielded significantly higher correlations than the linear model for all the neurovascular measures (all $|t|$'s$(61) > 4.825$, $p < .0001$). For both [HbO_2] and [HbR] the mean correlations with the square root of the integrated fast response were higher for the young ($r = .65$ for [HbO_2] and $r = -.68$ for [HbR]) than for the old subjects ($r = .37$ for [HbO_2] and $r = -.52$ for [HbR]). This effect was significant for [HbO_2], $t(61) = 2.23$, $p < .05$, but not for [HbR], $t(61) = 1.64$, n.s. No difference between younger and older adults was obtained when the integrated fast response was used to predict the BOLD response (mean $r = .79$ for younger adults and mean $r = .77$ for older adults, respectively), $t(61) < 1$.

Essentially identical results were obtained when using the ERP measures to estimate the neuronal response. As for the EROS-based prediction, the quadratic model performed significantly better than the linear model (all $|t|(62) > 2.89$, all p's$< .01$). For the quadratic model, the correlations of the predicted hemodynamic response with [HbO_2] and [HbR] were higher in the young (mean $r = .67$ for [HbO_2] and mean $r = -.67$ for [HbR]) than in the older adults (mean $r = .47$ for [HbO_2] and mean $r = -.51$ for [HbR]), $t(61) = 2.42$, $p < .05$, and $t(61) = -1.72$, $p < .10$, respectively. Similarly to the EROS-based estimates, no difference between the correlations for younger and older adults was obtained with the BOLD response

(mean *r*=.77 for the younger and *r*=.82 for the older adults). These data indicate that the hemodynamic response is better correlated with the square root of the integrated neuronal response than with the untransformed value. This suggests that, at least in visual cortex, the neurovascular relationship departs markedly from linearity and tends to generate a decelerated function with reduced increases in hemodynamic responses as a function of additional equal increases in the neuronal response. This was the case independently of the modality used to estimate the neuronal (EROS or ERPs) or the vascular response (NIRS or fMRI). In addition, the coupling between oxy- and deoxy-hemoglobin response decreases with aging at least in occipital regions, and there is some hint to a break-down of the neurovascular coupling in general in older adults, although this appears to depend on the hemodynamic variable used for the estimates.

Discussion

The data reported in this paper indicate that the relationship between neuronal (EROS, ERPs) and vascular (NIRS and BOLD) measures of brain function in the case of visual stimulation departs substantially from linearity in younger and older adults. In this respect, the data differ from previous reports obtained with optical methods (Gratton et al., 2001) and other techniques (e.g., Buckner et al, 2000; Dale & Buckner, 1997; D'Esposito et al., 1999; Huettel et al., 2001; Miezin et al. 2000; Pollman et al., 2001; Wobst et al., 2001), but are consistent with others suggesting a non-linear relationship (Arthurs et al., 2007; Binder et al., 1994; Birn et al., 2001; Friston et al., 1998; Hewson-Stoate et al., 2005; Jones et al., 2004; Liu & Gao, 2000; Rees et al., 1997; Sloan et al., 2010; Vazquez & Noll, 1998). Older adults also show, in general, a similar relationship to younger adults between neuronal and vascular measures when the BOLD fMRI and [HbR] responses are considered, although the amplitude of the component responses (both neuronal and hemodynamic) is somewhat depressed relative to that of the younger subjects. This confirms previous findings for visual areas (e.g., Buckner et al., 2000). However, for older adults a different picture emerges when [HbO_2] changes are taken into consideration. In this case, the neurovascular coupling is somewhat disrupted in the low-fit older adults, as demonstrated by the very reduced [HbO_2] response in this group – even though the neuronal response is equally large in the high-and low-fit subjects.

These age-related changes in neurovascular coupling are likely to reflect problems within the vascular system, which may emerge in aging. In fact, these changes appear particularly evident in subjects with low cardiorespiratory fitness. It should be noted that the older sample in our study was screened for a number of possible health problems. Specifically, no severe hypertension cases were included in our sample, and subjects were in sufficient good health to be able to complete the maximal graded exercise test. Nevertheless, the low-fit subjects in our study had, on average, higher blood pressure and higher body-mass index (BMI). Thus, it is likely that the reactivity of the vascular system in low-fit older adults was somewhat poorer than in those older adults with higher fitness levels and in the younger adults. A possible explanation for this phenomenon is that the vascular system of low-fit older adults may have lost some of its ability to adapt to increased task demands, with blood vessels already being dilated even during the rest conditions. Another possibility (which is not inconsistent with the previous account) is that low-fit older adults may have lost some of their brain capillary bed. This is consistent with the notion that aerobic exercise (which increases cardiorespiratory fitness) leads to an increase in angiogenesis (Isaacs et al., 1992) and thus increased perfusion.

The data presented here have important implications for functional imaging studies and for the interpretation of functional aging data. First, at least for visual cortex, they indicate that some caution should be taken when using linear decomposition methods, such as SPM or

fast event-related fMRI, in the analysis of hemodynamic imaging data, in particular from older adults, because the neurovascular coupling function shows signs of saturation at higher levels of neuronal activation. This non-linearity may be mediated in part by the different spatial extent of the neuronal and hemodynamic responses. In any case, these data indicate that caution should be taken when inferring neuronal activity from hemodynamic signals. Second, this is likely to be even more problematic in low-fit older adults, who show a depressed neurovascular response at least for measures of [HbO_2]. Third, the data indicate that fitness level is important for neuroimaging studies of aging. Specifically, they show that age-related reductions in hemodynamic brain responses (at least for [HbO_2] measures) may not reflect similar reductions in neuronal responses.

Several previous studies have compared hemodynamic responses in older adults with those of younger adults. Some of these studies have focused on the amplitude of the hemodynamic responses and typically suggest a depression of neurovascular coupling in older adults (D'Esposito et al., 1999; Hesselman et al., 2001; Huettel et al., 2001). However, some of these studies involved only hemodynamic measures. In this case, it is difficult to determine whether the observed differences had to be attributed to changes in neuronal function or changes in neurovascular coupling. Further, for the most part, the effects reported in these studies were quite variable across individuals, perhaps because fitness was not controlled for, and subjects could vary significantly with respect to this variable. The current experiment confirms the presence of a depression of neurovascular coupling in low-fit older adults and indicates that fitness may be an important source of individual differences, especially among the elderly.

The data indicate variability in the coupling of the [HbO] and [HbR] responses to stimulation as a function of aging. This finding is in line with that reported by Safonova et al. (2004). Specifically, older adults showed a low correlation between the two responses. This may in part be due to the fact that both responses were smaller in older than in younger adults, and therefore more difficult to measure on individual subjects. However, figure 7C also indicates that the compensatory vasodilation indexed by the BOLD response was reduced in older adults. In other words, the increase in blood flow may have been too small to lead to an increase in [HbO] in at least some of the older adults, as all the incoming oxygen may have been used up by the activated tissue.

This study also highlights the potential utility of optical imaging as a tool for studying neurovascular coupling. An advantage of optical imaging is that measurement of neuronal and hemodynamic parameters could be taken simultaneously. A further advantage is that these measures can be referred to specific brain regions, and that, in principle, given the appropriate paradigm and recording methods more than one region could be studied in parallel. This could be used to evaluate whether neurovascular coupling changes significantly with location within or across individuals or groups.

Although our study focused on optical measures, we also recorded ERP activity. The two modalities responded similarly to the frequency manipulation. They also showed a good correspondence in terms of latency of the response, and between the patterns of activities at different latencies in different age groups. However, the EROS measures were more highly correlated across groups with the hemodynamic measures than the ERPs. Two factors may account for this finding. First, the EROS response is more precisely localized than the ERP response, and therefore less susceptible to cross-talk from different brain regions. Second, just like the hemodynamic measures (BOLD fMRI and NIRS signals) the EROS response is related to scalar properties (scattering changes) of the activated area, whereas the ERP response is related to vectorial properties of the brain, and specifically to the orientation in space of the cortical region involved in its generation. If the orientation differs

systematically across subject populations, the relationship between ERPs and the hemodynamic measures may also vary. As a consequence, the slopes of the neurovascular function for different subject groups may not align.

The current study also had several limitations, which should lead to further investigation. First, only visual stimulation and occipital cortex were investigated. Further studies will need to be carried out to determine whether the finding of a non-linear relationship between neuronal and hemodynamic measures is generalizable to other cortical regions. Indeed, some investigators suggest that the relationship between neuronal and vascular measures might vary in different cortical regions (e.g., Huettel et al., 2004). Second, fitness was evaluated across individuals, in a correlational rather than experimental fashion. Recent work shows that aerobic exercise may result in changes in several functional parameters (Emery et al., 1998; Kharti et al., 2001; Kramer et al., 1999, 2001). It is likely that it may also lead to changes in neurovascular coupling. It is however also possible that fitness per se may not be the critical variable, but only a correlate of some other factors (e.g., genetic variations, nutrition) which may be more directly related to vascular health and neurovascular coupling. These variables may be studied independently and in combination to determine their relative influence on neurovascular coupling. Third, it is not clear from the current data whether the reduction in neurovascular coupling observed in the low-fit older adults has any functional counterpart. This is because the task used in the current study (passive viewing of a reversing checkerboard) did not result in any behavioral measure. To evaluate the functional impact of reduced neurovascular coupling it will be necessary to employ more informative behavioral manipulations, perhaps including tasks varying in difficulty. Fourth, we only used one way of manipulating the amplitude of the hemodynamic response in the current study (i.e., through variations in the stimulation frequency). It is possible that different rules would regulate neurovascular coupling when other manipulations are used, such as the duration of the stimulation or its intensity. This remains a subject for future investigation.

In conclusion, this study presents an investigation of neurovascular coupling in younger and older adults differing in fitness levels, based on optical imaging as well as electrophysiological and fMRI measures. The results indicate the presence of a non-linear relationship between neuronal and hemodynamic effects in younger adults and in older adults with higher fitness levels, and an alteration of the hemodynamic response in older adults with lower fitness levels. The study also illustrates an approach to the investigation of neurovascular coupling based on the use of hemodynamic and neuronal optical measures, which in the future could be extended to other cortical regions and help inform the interpretation of cognitive neuroscience data.

Acknowledgments

The work presented in this paper was supported by NIA grant #AG21887 to M. Fabiani and by NIMH grant #R56MH097973 to G. Gratton. We wish to thank Yukyung Lee, Katherine S. Morris, and Shawna Doerksen for help with data collection, and Stan Colcombe and Kirk Erickson for useful advice for the analysis of the fMRI data.

References

Adachi Usami E. Human visual system modulation transfer function measured by evoked potentials. Neuroscience Letters. 1981; 23:43–47. [PubMed: 7231815]

Arthurs OJ, Williams EJ, Carpenter TA, Pickard JD, Boniface SJ. Linear coupling between functional magnetic resonance imaging and evoked potential amplitude in human somatosensory cortex. Neuroscience. 2000; 101:803–806. [PubMed: 11113329]

Arthurs OJ, Donovan T, Spiegelhalter DJ, Pickard JD, Boniface SJ. Intracortically distributed neurovascular coupling relationships within and between human somatosensory cortices. Cerebral Cortex. 2007; 17:661–668. [PubMed: 16648455]

Beck, AT.; Steer, RA.; Brown, GK. Manual for the Beck Depression Inventory. 2nd Ed. San Antonio, TX: The Psychological Corporation; 1996.

Binder JR, Rao SM, Hammeke TA, Frost JA, Bandettini PA, Hyde JS. Effects of stimulus rate on signal response during functional magnetic resonance imaging of auditory cortex. Brain Research. Cognitive Brain Research. 1994; 2:31–38. [PubMed: 7812176]

Birn RM, Saad ZS, Bandettini PA. Spatial heterogeneity of the nonlinear dynamics in the fmri bold response. NeuroImage. 2001; 14:817–826. [PubMed: 11554800]

Black JE, Isaacs KR, Anderson BJ, Alcantara AA, Greenough WT. Learning causes synaptogenesis, whereas motor activity causes angiogenesis, in cerebellar cortex of adult rats. Proceedings of the National Academy of Sciences U S A. 1990; 87:5568–5572.

Boas DA, Gaudette T, Strangman G, Cheng X, Marota JJA, Mandeville JB. The accuracy of near infrared spectroscopy and imaging during focal changes in cerebral hemodynamics. NeuroImage. 2001; 13:76–90. [PubMed: 11133311]

Buckner RL, Snyder AZ, Sanders AI, Raichle ME, Morris JC. Functional brain imaging of young, nondemented, and demented older adults. Journal of Cognitive Neuroscience, Supplement 2. 2000; 12:24–34.

Buxton RB, Uludag K, Dubowitz DJ, Liu TT. Modeling the hemodynamic response to brain activation. Neuroimage. 2004; 23:S220–S233. [PubMed: 15501093]

Cabeza R. Hemispheric asymmetry reduction in older adults: the HAROLD model. Psychology and Aging. 2002; 17:85–100. [PubMed: 11931290]

Colcombe SJ, Erickson KI, Raz N, Webb AG, Cohen NJ, McAuley E, Kramer AF. Aerobic fitness reduces brain tissue loss in aging humans. Journal of Gerontology: Medical Sciences. 2003; 58:176–180.

Colcombe SJ, Erickson KI, Scalf PE, Kim JS, Prakash R, McAuley E, Elavsky S, Marquez DX, Hu L, Kramer AF. Aerobic exercise training increases brain volume in aging humans. Journal of Gerontology: Medical Sciences. 2006; 61:1166–1170.

Colcombe S, Kramer AF. Fitness effects on the cognitive function of older adults: A meta-analytic study. Psychological Science. 2003; 14:125–130. [PubMed: 12661673]

Cotman CW, Berchtold NC, Christie LA. Exercise builds brain health: Key roles of growth factor cascades and inflammation. Trends in Neuroscience. 2007; 30(9):464–472.

Chiarelli AM, Di Vacri A, Romani GL, Merla A. Fast optical signal in visual cortex: Improving detection by General Linear Convolution Model. NeuroImage. 2012; 66:194–202. [PubMed: 23110889]

Cope M, Delpy DT. System for long-term measurement of cerebral blood and tissue oxygenation of newborn infants by near infra-red transillumination. Medical and Biological Engineering and Computing. 1988; 26:289–294. [PubMed: 2855531]

Cox RW. AFNI: Software for analysis and visualization of functional magnetic resonance neuroimages. Computers and Biomedical Research. 1996; 29:162–173. [PubMed: 8812068]

Dale AM, Buckner RL. Selective averaging of rapidly presented individual trials using fMRI. Human Brain Mapping. 1997; 5:329–340. [PubMed: 20408237]

DeSoto MC, Fabiani M, Geary DL, Gratton G. When in doubt, do it both ways: Brain evidence of the simultaneous activation of conflicting responses in a spatial Stroop task. Journal of Cognitive Neuroscience. 2001; 13:523–536. [PubMed: 11388924]

D'Esposito M, Deouell LY, Gazzaley A. Alterations in the BOLD fMRI signal with ageing and disease: a challenge for neuroimaging. Nature Review: Neuroscience. 2003; 4:863–872.

D'Esposito M, Zarahan E, Aguirre GK, Rympa B. The effect of normal aging on the coupling of neural activity to the bold hemodynamic response. Neuroimage. 1999; 10:6–14. [PubMed: 10385577]

Dustman RE, Ruhling RO, Russell RM, Shearer DE, Bonekat HW, Shigeoka JW, Woods JS, Bradford DC. Aerobic exercise training and improved neuropsychological function of older individuals. Neurobiology of Aging. 1984; 5:35–42. [PubMed: 6738784]

Emery CF, Schein RL, Hauck ER, MacIntyre NR. Psychological and cognitive outcomes of a randomized trial of exercise among patients with chronic obstructive pulmonary disease. Health Psychology. 1998; 17:232–240. [PubMed: 9619472]

Erickson KI, Prakash RS, Voss MW, Chaddock L, Hu L, Morris KS, White SM, Wojcicki TR, McAuley E, Kramer AF. Aerobic fitness is associated with hippocampal volume in elderly humans. Hippocampus. in press

Erickson KI, Voss M, Prakash R, Basak C, Chaddock L, Kim J, Heo S, Alves H, White S, Wojcicki T, Mailey E, Vieira V, Martin S, Pence B, Woods J, McAuley E, Kramer AF. Exercise training increases size of hippocampus and improves memory. Proceedings of the National Academy of Sciences. 2011; 108(7):3017–3022.

Fabiani M, Low KA, Wee E, Sable JJ, Gratton G. Reduced suppression or labile memory? Mechanisms of inefficient filtering of irrelevant information in older adults. Journal of Cognitive Neuroscience. 2006; 18:637–650. [PubMed: 16768366]

Fox PT, Raichle ME. Stimulus rate determines regional brain blood flow in striate cortex. Annals of Neurology. 1985; 17:303–305. [PubMed: 3873210]

Franceschini MA, Boas DA. Noninvasive measurement of neuronal activity with near-infrared optical imaging. NeuroImage. 2004; 21:372–386. [PubMed: 14741675]

Franceschini MA, Nissilä I, Wu W, Diamond SG, Bonmassar G, Boas DA. Coupling between somatosensory evoked potentials and hemodynamic response in the rat. NeuroImage. 2008; 41(2): 189–203. [PubMed: 18420425]

Friston KJ, Fletcher P, Josephs O, Holmes A, Rugg MD, Turner R. Event-related fMRI: Characterizing differential responses. Neuroimage. 1998; 7:30–40. [PubMed: 9500830]

Friston KJ, Holmes AP, Poline JB, Grasby PJ, Williams SC, Frackowiak RS, Turner R. Analysis of fMRI time-series revisited. Neuroimage. 1995; 2(1):45–53. [PubMed: 9343589]

Gazzaley A, Cooney JW, Rissman J, D'Esposito M. Top-down suppression deficit underlies working memory impairment in normal aging. Nature Neuroscience. 2005; 8(10):1298–1300. Erratum in: Nature Neuroscience. 8(12):1791.

Gordon B, Rykhlevskaia E, Brumback CR, Lee Y, Elavsky S, Konopack JF, McAuley E, Kramer AF, Colcombe S, Gratton G, Fabiani M. Anatomical correlates of aging, cardiopulmonary fitness level, and education. Psychophysiology. 2008; 45:825–838. [PubMed: 18627534]

Gratton G, Brumback CR, Gordon BA, Pearson MA, Low KA, Fabiani M. Effects of measurement method, wavelength, and source-detector distance on the fast optical signal. NeuroImage. 2006; 32:1576–1590. [PubMed: 16872842]

Gratton G, Coles MGH, Donchin E. A new method for off-line removal of ocular artifact. Electroencephalography and Clinical Neurophysiology. 1983; 55:468–484. [PubMed: 6187540]

Gratton G, Corballis PM. Removing the heart from the brain: Compensation for the pulse artifact in the photon migration signal. Psychophysiology. 1995; 32:292–299. [PubMed: 7784538]

Gratton G, Corballis PM, Cho E, Fabiani M, Hood D. Shades of gray matter: Noninvasive optical images of human brain responses during visual stimulation. Psychophysiology. 1995; 32:505–509. [PubMed: 7568645]

Gratton G, Fabiani M. Shedding light on brain function: The event-related optical signal. Trends in Cognitive Sciences. 2001; 5:357–363. [PubMed: 11477005]

Gratton G, Fabiani M. The event-related optical signal, EROS) in visual cortex: Replicability, consistency, localization and resolution. Psychophysiology. 2003; 40:561–571. [PubMed: 14570164]

Gratton G, Fabiani M, Corballis PM, Hood DC, Goodman-Wood MR, Hirsch J, Kim K, Friedman D, Gratton E. Fast and localized event-related optical signals, EROS) in the human occipital cortex: Comparison with the visual evoked potential and fMRI. NeuroImage. 1997; 6:168–180. [PubMed: 9344821]

Gratton G, Goodman-Wood MR, Fabiani M. Comparison of neuronal and hemodynamic measure of the brain response to visual stimulation: an optical imaging study. Human Brain Mapping. 2001; 13:13–25. [PubMed: 11284043]

Gratton G, Sarno AJ, Maclin E, Corballis PM, Fabiani M. Toward non-invasive 3-D imaging of the time course of cortical activity: Investigation of the depth of the event-related optical signal, EROS. NeuroImage. 2000; 11:491–504. [PubMed: 10806035]

Hesselmann V, Zaro Weber O, Wedekind C, Krings T, Schulte O, Kugel H, Krug B, Klug N, Lackner KJ. Age related signal decrease in functional magnetic resonance imaging during motor stimulation in humans. Neuroscience Letters. 2001; 10:141–144. [PubMed: 11479008]

Hewson-Stoate N, Jones M, Martindale J, Berwick J, Mayhew J. Further nonlinearities in neurovascular coupling in rodent barrel cortex. NeuroImage. 2005; 24:565–574. [PubMed: 15627599]

Huettel SA, Singerman JD, McCarthy G. The effects of aging upon the hemodynamic response measured by functional MRI. NeuroImage. 2001; 13:161–175. [PubMed: 11133319]

Huettel SA, McKeown MJ, Song AW, Hart S, Spencer DD, Allison T, McCarthy G. Linking hemodynamic and electrophysiological measures of brain activity: Evidence from functional MRI and intracranial field potentials. Cerebral Cortex. 2004; 14:165–173. [PubMed: 14704213]

Joanna K, Huttunen JK, Gröhn O, Penttonen M. Coupling between simultaneously recorded BOLD response and neuronal activity in the rat somatosensory cortex. NeuroImage. 2008; 39:775–785. [PubMed: 17964186]

Isaacs KR, Anderson BJ, Alcantara AA, Black JE, Greenough WT. Exercise and the brain: angiogenesis in the adult rat cerebellum after vigorous physical activity and motor skill learning. Journal of Cerebral Blood Flow and Metabolism. 1992; 12:110–119. [PubMed: 1370068]

Jones M, Hewson-Stoate N, Martindale J, Redgrave P, Mayhew J. Nonlinear coupling of neural activity and CBF in rodent barrel cortex. NeuroImage. 2004; 22:956–965. [PubMed: 15193627]

Kato T, Kamei A, Takashima S, Ozaki T. Human visual cortical function during photic stimulation monitoring by means of near-infrared spectroscopy. Journal of Cerebral Blood Flow and Metabolism. 1993; 13:516–520. [PubMed: 8478409]

Kharti P, Blumenthal JA, Babyak MA, Craighead WE, Herman S, Baldewicz T, Madden DJ, Doraiswamy M, Waugh R, Krishman KR. Effects of exercise training on cognitive functioning among depressed older men and women. Journal of Aging and Physical Activity. 2001; 9:43–57.

Kramer, AF.; Fabiani, M.; Colcombe, S. Contributions of cognitive neuroscience to the understanding of behavior and aging. In: Birren, JE.; Schaie, KW., editors. Handbook of the Psychology of Aging, Sixth Edition. New York, NY: Academic Press; 2006. p. 57-83.

Kramer AF, Hahn S, Cohen N, Banich M, McAuley E, Harrison C, Chason J, Vakil E, Bardell L, Boileau RA, Colcombe A. Aging, fitness, and neurocognitive function. Nature. 1999; 400:418–419. [PubMed: 10440369]

Kramer, AF.; Hahn, S.; McAuley, E.; Cohen, NJ.; Banich, MT.; Harrison, C.; Chason, J.; Boileau, RA.; Bardell, L.; Colcombe, A.; Vakil, E. Exercise, aging and cognition: Healthy body, healthy mind?. In: Fisk, AD.; Rogers, W., editors. Human factors interventions for the health care of older adults. Hillsdale, N.J.: Erlbaum; 2001.

Kubota M, Inouchi M, Dan I, Tsuzuki D, Ishikawa A, Scovel T. Fast, 100–175 ms) components elicited bilaterally by language production as measured by three-wavelength optical imaging. Brain Research. 2008; 1226:124–33. [PubMed: 18573241]

Lin FH, McIntosh AR, Agnew JA, Eden GF, Zeffiro TA, Belliveau JW. Multivariate analysis of neuronal interactions in the generalized partial least squares framework: simulations and empirical studies. NeuroImage. 2003; 20:625–642. [PubMed: 14568440]

Liu H, Gao J. An investigation of the impulse functions for the nonlinear BOLD response in functional MRI. Magnetic Resonance Imaging. 2000; 18:931–938. [PubMed: 11121695]

Logothetis NK, Pauls J, Augath M, Trinath T, Oeltermann A. Neurophysiological investigation of the basis of the fMRI signal. Nature. 2001; 412:150–157. [PubMed: 11449264]

Mackert B-M, Leistnera S, Sander T, Liebert A, Wabnitz H, Burghoff M, Trahms L, Macdonald R, Curio G. Dynamics of cortical neurovascular coupling analyzed by simultaneous DC-magnetoencephalography and time-resolved near-infrared spectroscopy. NeuroImage. 2008; 39:979–986. [PubMed: 17997330]

Mackert B-M, Wübbeler G, Leistner S, Uludag K, Obrig H, Villringer A, Trahms L, Curio G. Neurovascular coupling analyzed non-invasively in the human brain. Neuroreport. 2004; 15:63–66. [PubMed: 15106832]

Martínez A, Anllo-Vento L, Sereno MI, Frank LR, Buxton RB, Dubowitz DJ, Wong EC, Hinrichs H, Heinze HJ, Hillyard SA. Involvement of striate and extrastriate visual cortical areas in spatial attention. Nature Neuroscience. 1999; 2:364–369.

Mayeux R, Stern Y, Rosen J, Leventhal J. Depression, intellectual impairment and Parkinson's disease. Neurology. 1981; 31:645–650. [PubMed: 7195481]

Medvedev AV, Kainerstorfer J, Borisov SV, Barbour RL, VanMeter J. Event-related fast optical signal in a rapid object recognition task: improving detection by the independent component analysis. Brain Research. 2008; 1236:145–158. [PubMed: 18725213]

Menon RS, Kim SG. Spatial and temporal limits in cognitive neuroimaging with fMRI. Trends in Cognitive Sciences. 1999; 3:207–216. [PubMed: 10354573]

Miezin FM, Maccotta L, Ollinger JM, Petersen SE, Buckner RL. Characterizing the hemodynamic response: Presentation rate, sampling procedure, and the possibility of ordering brain activity based on relative timing. NeuroImage. 2000; 11:735–759. [PubMed: 10860799]

Miller J, Patterson T, Ulrich R. Jackknife-based method for measuring LRP onset latency differences. Psychophysiology. 1998; 35:99–115. [PubMed: 9499711]

Obrig H, Israel H, Kohl-Bareis M, Uludag K, Wenzel R, Müller B, Arnold G, Villringer A. Habituation of the visually evoked potential and its vascular response: implications for neurovascular coupling in the healthy adult. Neuroimage. 2002; 17(1):1–18. [PubMed: 12482064]

Niehaus L, Lehmann R, Röricht S, Meyer B-U. Age-related reduction in visually evoked cerebral blood flow responses. Neurobiology of Aging. 2001; 22:35–38. [PubMed: 11164274]

Ou W, Nissilä I, Radhakrishnan H, Boas DA, Hämäläinen MS, Franceschini MA. Study of neurovascular coupling in humans via simultaneous magnetoencephalography and diffuse optical imaging acquisition. NeuroImage. 2009; 46:624–632. [PubMed: 19286463]

Parks NA, Maclin EL, Low KA, Beck DM, Fabiani M, Gratton G. Examining Cortical Dynamics and Connectivity with Concurrent Simultaneous Single-Pulse Transcranial Magnetic Stimulation and Fast Optical Imaging. NeuroImage. 2012; 59(3):2504–3510. [PubMed: 21925608]

Pollmann S, Dove A, Yves von Cramon D, Wiggins CJ. Event-related fMRI: Comparison of conditions with varying BOLD overlap. Human Brain Mapping. 2000; 9:26–37. [PubMed: 10643727]

Radhakrishnan H, Vanduffel W, Deng HP, Leeland E, Boas DA, Franceschini MA. Fast optical signal not detected in awake behaving monkeys. NeuroImage. 2009; 45:410–419. [PubMed: 19150500]

Raz N, Lindenberger U, Rodrigue KM, Kennedy KM, Head D, Williamson A, Dahle C, Gerstorf D, Acker JD. Regional brain changes in aging healthy adults: general trends, individual differences and modifiers. Cerebral Cortex. 2005; 15(11):1676–1689. [PubMed: 15703252]

Raz N, Rodrigue KM, Haacke EM. Brain aging and its modifiers: insights from in vivo neuromorphometry and susceptibility weighted imaging. Annals of the NY Academy of Sciences. 2007; 1097:84–93.

Rees G, Howseman A, Josephs O, Frith CD, Friston KJ, Frackowiak RS, Turner R. Characterizing the relationship between BOLD contrast and regional cerebral blood flow measurements by varying the stimulus presentation rate. NeuroImage. 1997; 6:270–278. [PubMed: 9417970]

Reuter-Lorenz PA, Jonides J, Smith EE, Hartley A, Miller A, Marshuetz C, Koeppe RA. Age differences in the frontal lateralization of verbal and spatial working memory revealed by PET. Journal of Cognititve Neuroscience. 2000; 12:174–187.

Rinne T, Gratton G, Fabiani M, Cowan N, Maclin E, Stinard A, Sinkkonen J, Alho K, Näätänen R. Scalp-recorded optical signals make sound processing from the auditory cortex visible. NeuroImage. 1999; 10:620–624. [PubMed: 10547339]

Rosa MJ, Kilner J, Blankenburg F, Josephs O, Penny W. Estimating the transfer function from neuronal activity to BOLD using simultaneous EEG-fMRI Neuroimage. 2010 Jan 15; 49(2):1496–1509.

Rosen BR, Buckner RL, Dale AM. Event-related functional MRI: Past, present, and future. Proceedings of the National Academy of Sciences of the United States of America. 1998; 95:773–780. [PubMed: 9448240]

Rosengarten B, Aldinger C, Spiller A, Kaps M. Neurovascular coupling remains unaffected during normal aging. Journal of Neuroimaging. 2006; 13:43–47. [PubMed: 12593130]

Rykhlevskaia E, Fabiani M, Gratton G. Lagged covariance structure models for studying functional connectivity in the brain. NeuroImage. 2006; 30:1203–1218. [PubMed: 16414282]

Safonova KP, Michalos A, Wolf U, Wolf M, Hueber DM, Choi JA, Gupta R, Polzonetti C, Mantulin WW, Gratton E. Age-correlated changes in cerebral hemodynamics assessed by near-infrared spectroscopy. Archives of Gerontology and Geriatrics. 2004; 39:207–225. [PubMed: 15381340]

Salat DH, Buckner RL, Snyder AZ, Greve DN, Desikan RSR, Busa E, Morris JC, Dale AM, Fischl B. Thinning of the Cerebral Cortex in Aging. Cerebral Cortex. 2004; 14:721–730. [PubMed: 15054051]

Sloan HL, Austin VC, Blamire AM, Schnupp JWH, Lowe AS, Allers KA, Matthews PM, Sibson NR. Regional differences in neurovascular coupling in rat brain as determined by fMRI and electrophysiology. NeuroImage. 2010; 53(2010):399–411. [PubMed: 20633665]

Smith SM, Jenkinson M, Woolrich MW, Beckmann CF, Behrens TEJ, Johansen-Berg H, Bannister PR, De Luca M, Drobnjak I, Flitney DE, Niazy R, Saunders J, Vickers J, Zhang Y, De Stefano N, Brady JM, Matthews PM. Advances in functional and structural MR image analysis and implementation as FSL. NeuroImage. 2004; 23:208–219.

Steinbrink J, Kohl M, Obrig H, Curio G, Syré F, Thomas F, Wabnitz H, Rinneberg H, Villringer A. Somatosensory evoked fast optical intensity changes detected non-invasively in the adult human head. Neuroscience Letters. 2000; 291:105–108. [PubMed: 10978585]

Steinbrink J, Kempf FCD, Villringer A, Obrig H. The fast optical signal—Robust or elusive when non-invasively measured in the human adult? NeuroImage. 2005; 26:996–1008. [PubMed: 15961042]

Tse C-Y, Lee C-L, Sullivan J, Garnsey S, Dell GS, Fabiani M, Gratton G. Imaging the cortical dynamics of language processing with the Event-Related Optical Signal, EROS. Proceedings of the National Academy of Science USA. 2007; 104:17157–17162.

Van der Tweel LH, Verduyn Lunel HFE. Human visual responses to sinusoidally modulated light. Electroencephalography and Clinical Neurophysiology. 1965; 18:587–598. [PubMed: 14296836]

Vazquez AL, Noll DC. Nonlinear aspects of the BOLD response in functional MRI. NeuroImage. 1998; 7:108–118. [PubMed: 9558643]

Villringer A, Chance B. Non-invasive optical spectroscopy and imaging of human brain function. Trends in Neurosciences. 1997; 20:435–442. [PubMed: 9347608]

Wan X, Riera J, Iwata K, Takahashi M, Wakabayashi T, Kawashima R. The neural basis of the hemodynamic response nonlinearity in human primary visual cortex: Implications for neurovascular coupling mechanism. NeuroImage. 2006; 32(2):616–625. [PubMed: 16697664]

Washburn RA, Smith KW, Jette AM, Janney CA. The physical activity scale for the elderly, PASE): Development and evaluation. Journal of Clinical Epidemiology. 1993; 46:153–162. [PubMed: 8437031]

Wechsler, D. Wechsler Adult Intelligence Scale-Revised. San Antonio, TX: The Psychological Corporation; 1981.

Wobst P, Wenzel R, Kohl M, Obrig H, Villringer A. Linear aspects of changes in deoxygenated hemoglobin concentration and cytochrome oxidase oxidation during brain activation. NeuroImage. 2001; 13:520–530. [PubMed: 11170817]

Wolf U, Wolf M, Toronov V, Michalos A, Paunescu LA, Gratton E. Detecting cerebral functional slow and fast signals by frequency-domain near-infrared spectroscopy using two different sensors. Optical Society of America Biomedical Topical Meeting, Technical Digest. 2000:427–429.

Wolf M, Wolf U, Choi JH, Gupta R, Safonova LP, Paunescu LA, Michalos A, Gratton E. Functional frequency-domain near-infrared spectroscopy detects fast neuronal signal in the motor cortex. NeuroImage. 2002; 17:1868–1875. [PubMed: 12498761]

Zaletel M, Strucl M, Pretnar-Oblak J, Zvan B. Age-related changes in the relationship between visual evoked potentials and visually evoked cerebral blood flow velocity response. Functional Neurology. 2005; 20:15–20. [PubMed: 15948562]

Zhang, X.; Toronov, VY.; Fabiani, M.; Gratton, G.; Webb, AG. The study of cerebral hemodynamic and neuronal response to visual stimulation using simultaneous NIR optical tomography and BOLD fMRI in humans. In: Bartels, KE.; Bass, LS.; de Riese, WT.; Gregory, KW.; Hirschberg, H.; Katzir, A.; Kollias, N.; Madsen, SJ.; Malek, RS.; McNally-Heintzelman, KM.; Tate, LP., Jr;

Trowers, EA.; Wong, BJ-F., editors. Photonic Therapeutics and Diagnostics. Vol. Vol. 5686. 2005. p. 566-572.Proc. SPIE

Highlights

- Neurovascular coupling estimated in young and old adults varying in fitness level
- Measurements include neuronal (ERPs, EROS) and hemodynamic (fMRI, NIRS) methods
- Non-linear relationship was found between neuronal and hemodynamic measures
- Oxy-hemoglobin concentration changes were reduced in low-fit older adults

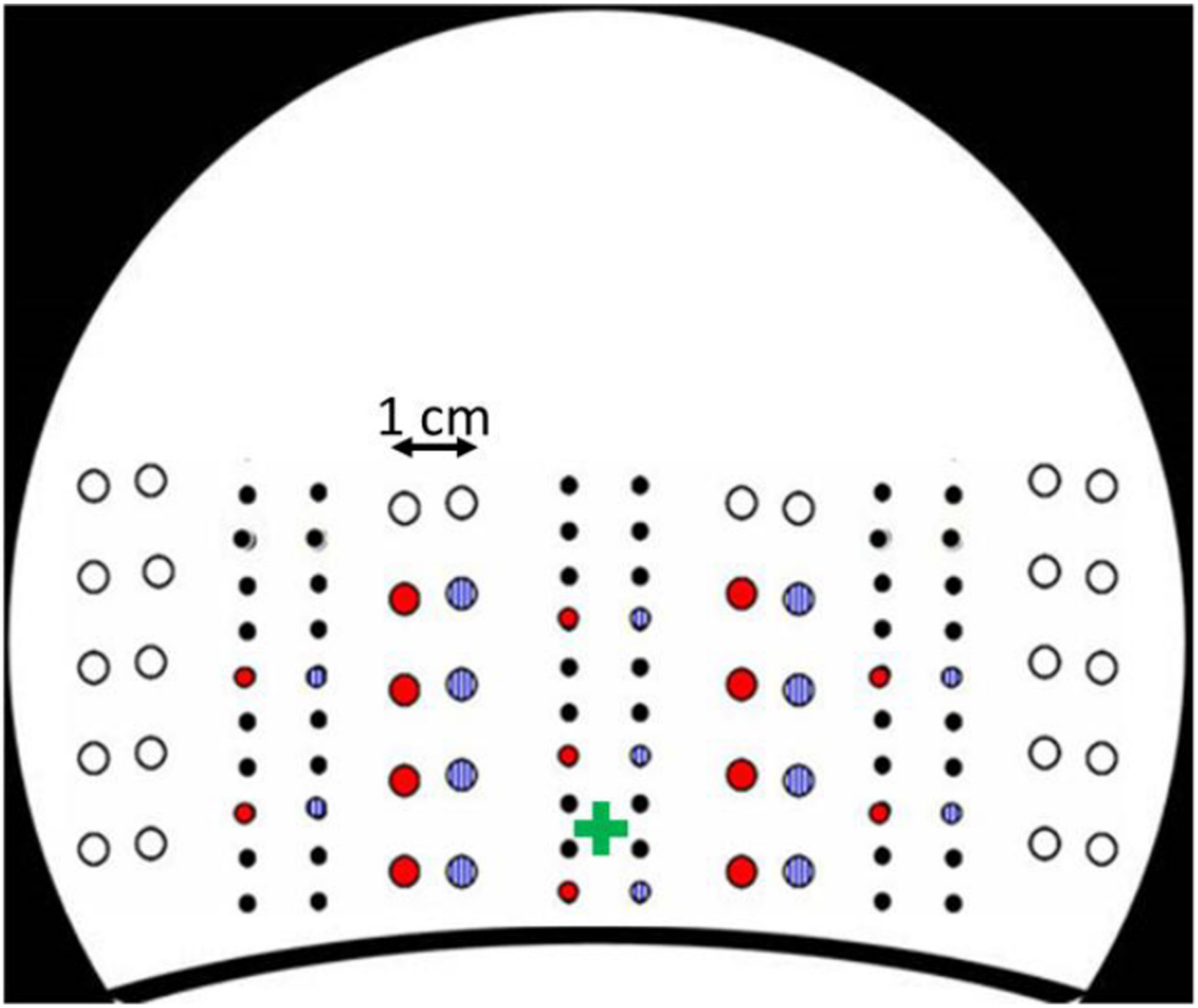

Figure 1.
Positions of the sources and detectors used in the study. Large circles represent detectors and small circles sources. Red and blue colors represent the two recording montages. The graph shows a schematic back view of the recording helmet. The approximate position of the inion is marked by a green cross.

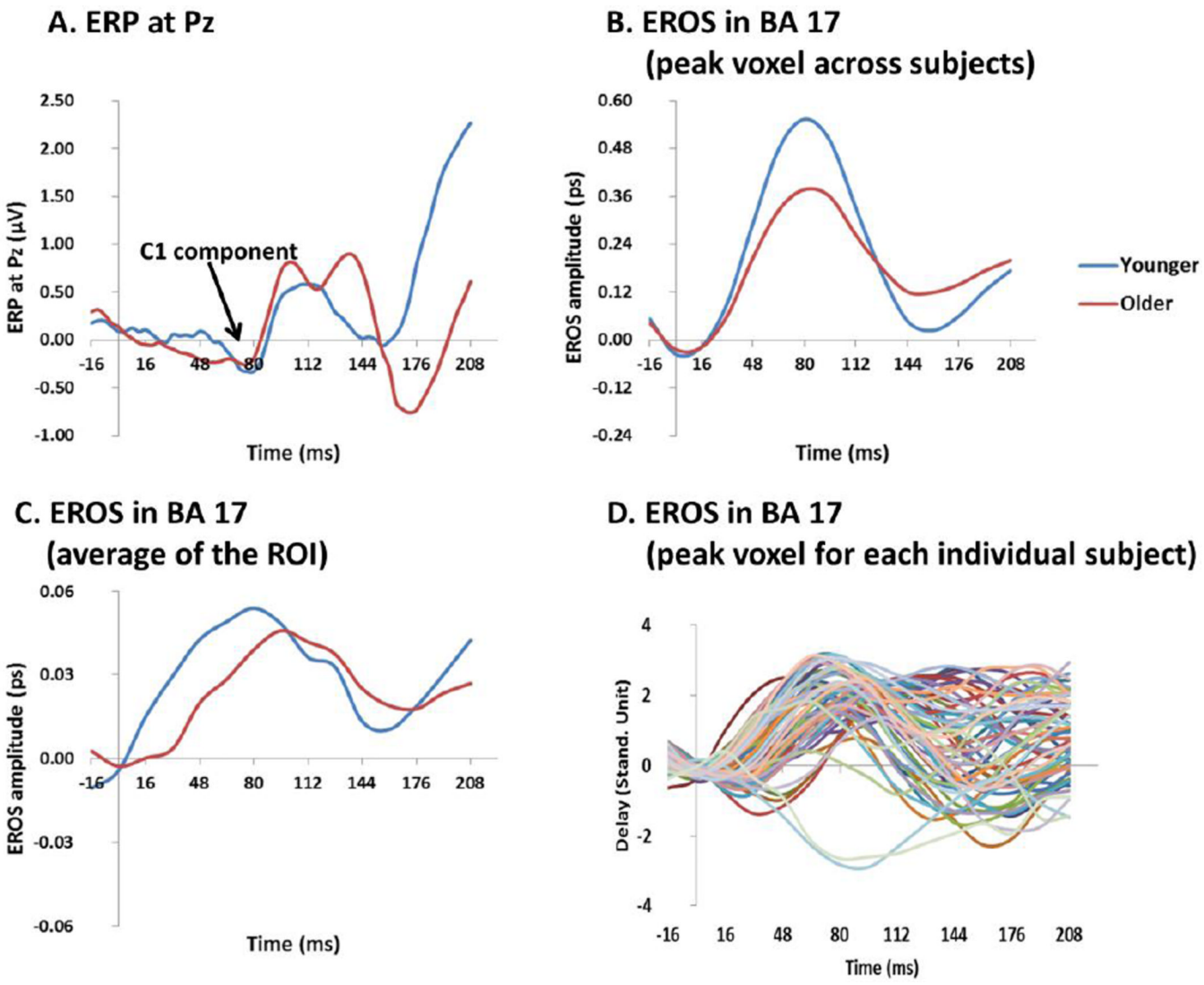

Figure 2.

(A) Time courses of the ERP response at the Pz electrode averaged across subjects (separately for each age group) and stimulation frequency conditions. (B) Grand average time courses across stimulation conditions of the EROS response at the *peak voxel across subjects* (same location across age groups) in the BA17 ROI; (C) Grand average time courses of the EROS response for the BA17 ROI, averaged across subjects (separately for each age group), stimulation conditions, and ROI voxels. (D) Time course of the standardized EROS response for each subject (averaged across stimulation conditions) at *each individual subject's peak location* within the BA17 ROI.

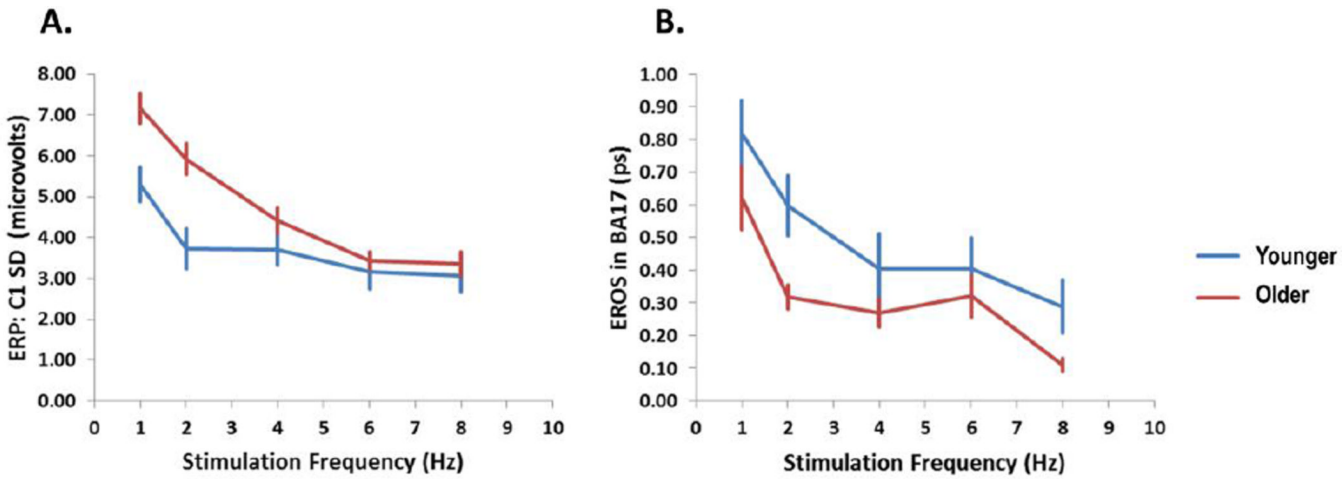

Figure 3.

(A) Amplitude of the ERP (SD of the C1 amplitude across electrodes in microvolts) and (B) amplitude of the peak EROS in BA17 (ps) responses, averaged across subjects, as a function of stimulation frequency, separately for younger and older adults. The error bars represent standard errors of the mean computed across subjects.

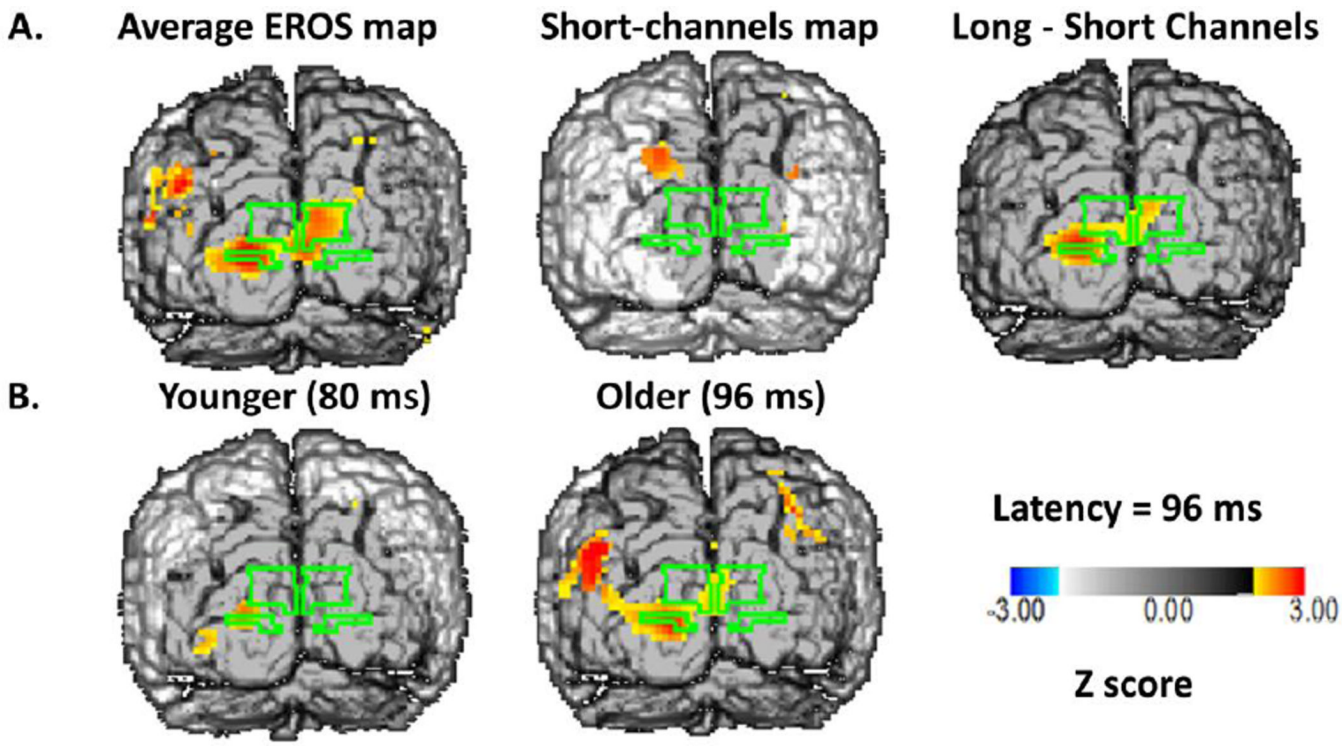

Figure 4.

A: Z-score maps of the EROS data at a latency of 96 ms after stimulation, averaged across all subjects and stimulation conditions. The surface projection of BA17 is outlined in green on each of the maps. **Left**: Average map across all subjects for source-detector distances between 20 and 50 mm. **Middle**: Average map across all subjects for source-detector distances between 0 and 17.5 mm (control condition). **Right**: Difference between the other two maps. **B**: Average Z-score maps of the EROS data for younger (left) and older (middle) adults.

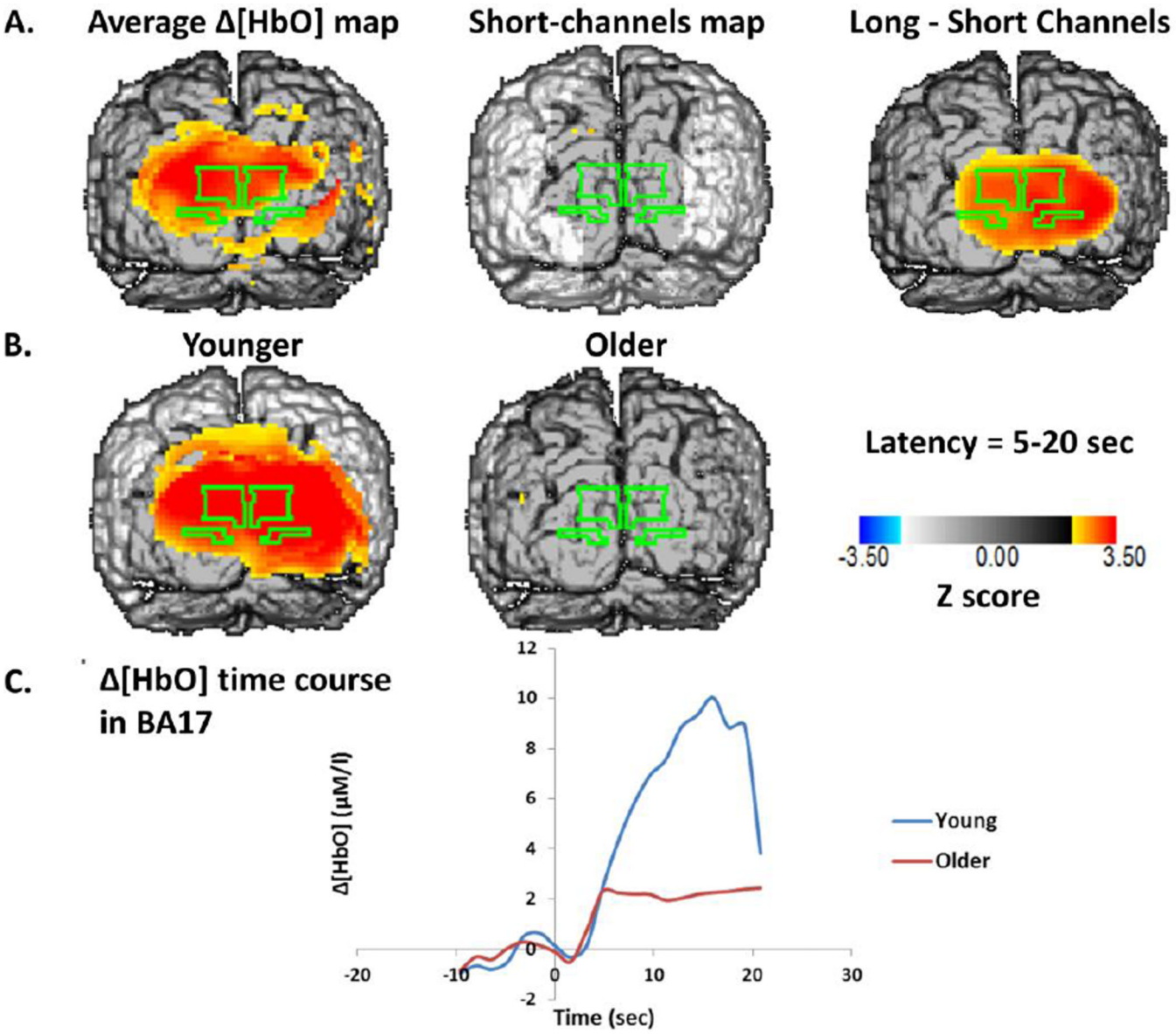

Figure 5.

A: Z-score maps of the [HbO_2] values between 5 and 15 seconds after the onset of stimulation. The surface projection of BA17 is outlined in green on each of the maps. **Left**: Average map across all subjects for source-detector distances between 20 and 50 mm. **Middle**: Average map across all subjects for source-detector distances between 0 and 17.5 mm (control condition). **Right**: Difference between the other two maps. **B**: Average Z-score maps of the [HbO_2] data for young (left) and older (middle) adults. **C**: Average time course across all voxels of BA17 for young and older subjects.

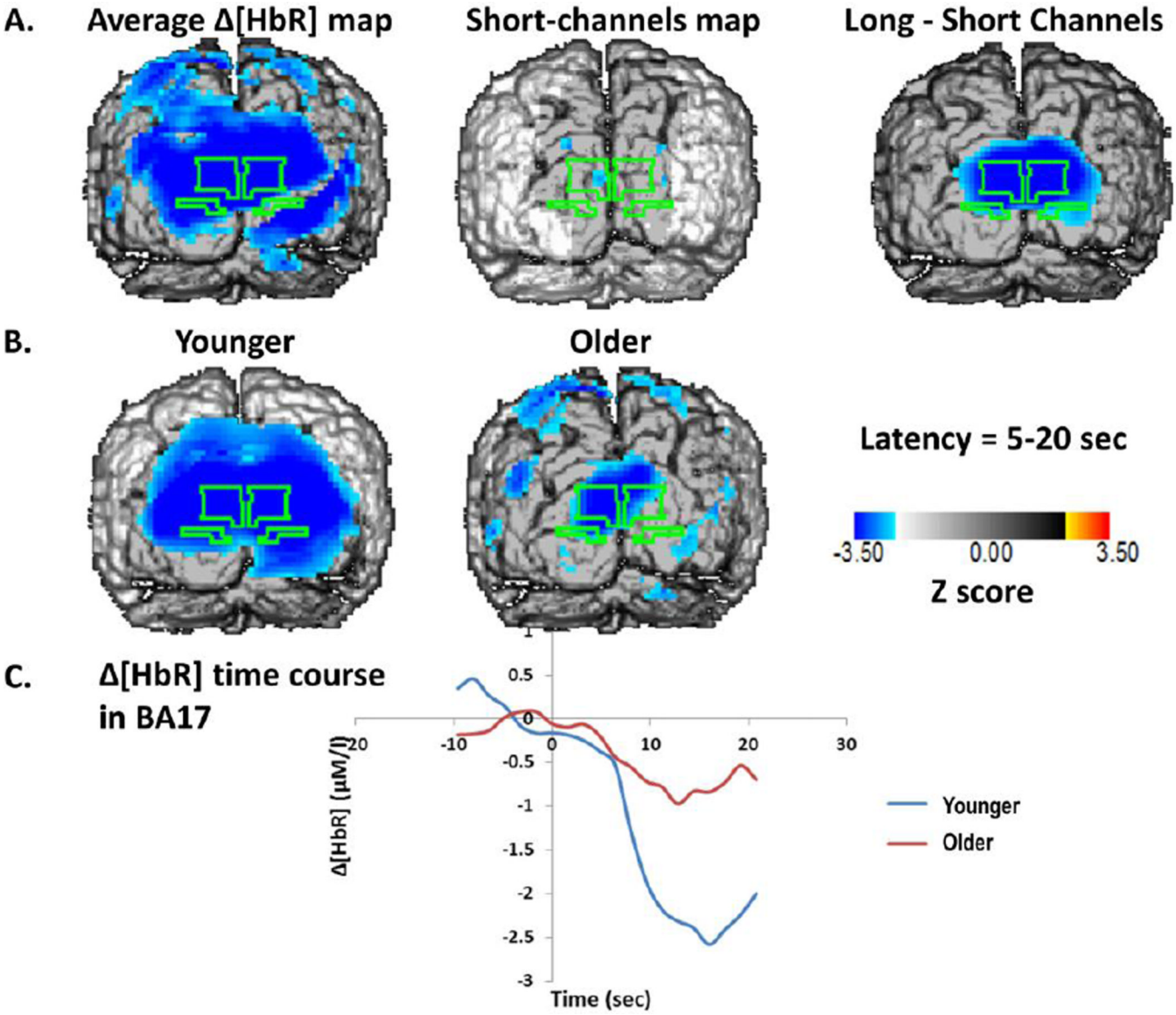

Figure 6.

A: Z-score maps of the [HbR] values between 5 and 15 seconds after the onset of stimulation. The surface projection of BA17 is outlined in green on each of the maps. **Left**: Average map across all subjects for source-detector distances between 20 and 50 mm. **Middle**: Average map across all subjects for source-detector distances between 0 and 17.5 mm (control condition). **Right**: Difference between the other two maps. **B**: Average Z-score maps of the [HbR] data for young (left) and older (middle) adults. **C**: Average time course across all voxels of BA17 for young and older subjects.

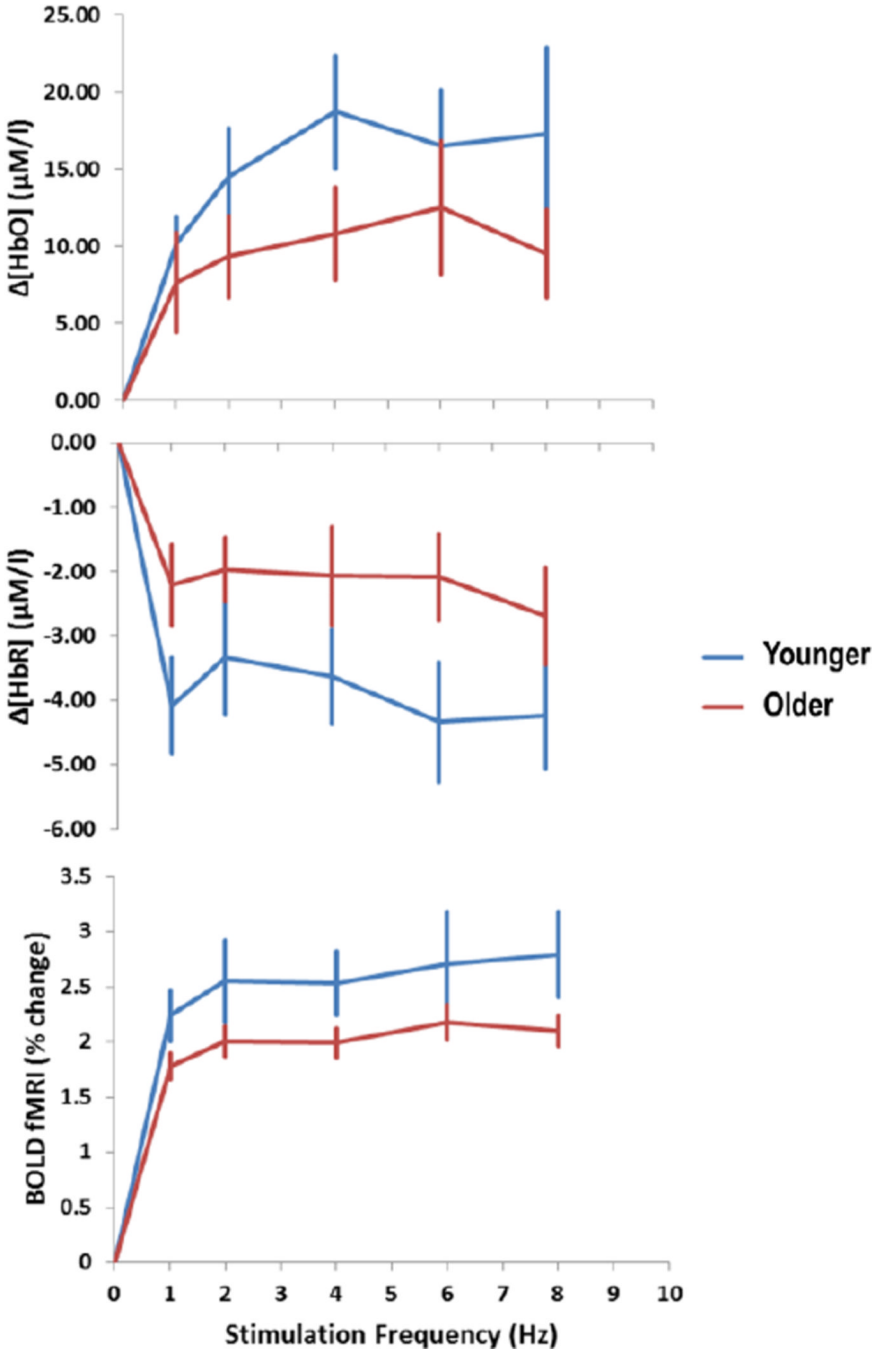

Figure 7.
Changes in hemodynamic parameters in BA17 during the stimulation period with respect to baseline, as a function of stimulation frequency and age group. The vertical bars indicate standard errors of the means computed across subjects.

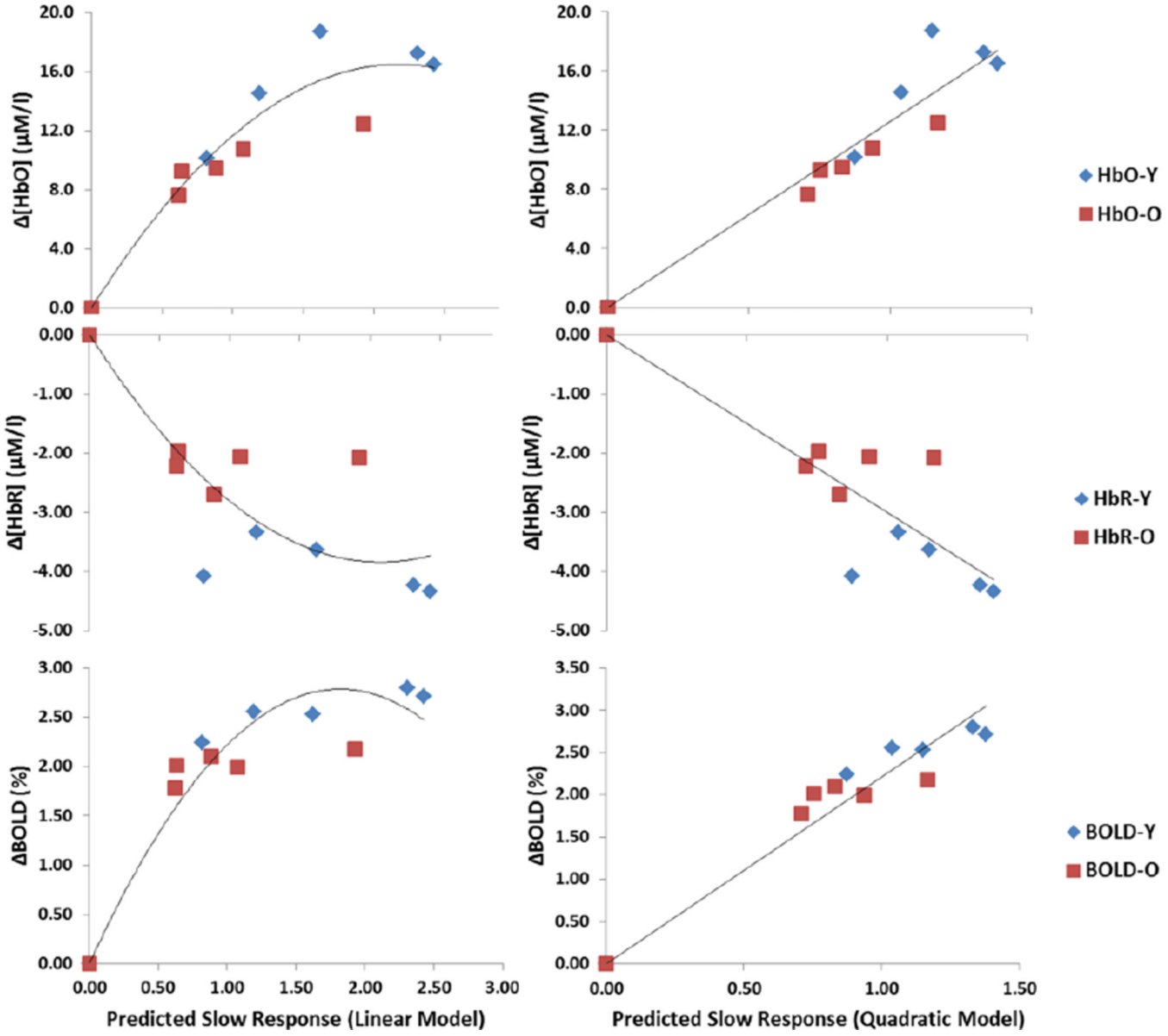

Figure 8.
Scatter plots depicting the relationships between the predicted and observed hemodynamic responses for each stimulation condition (averaged across subjects).

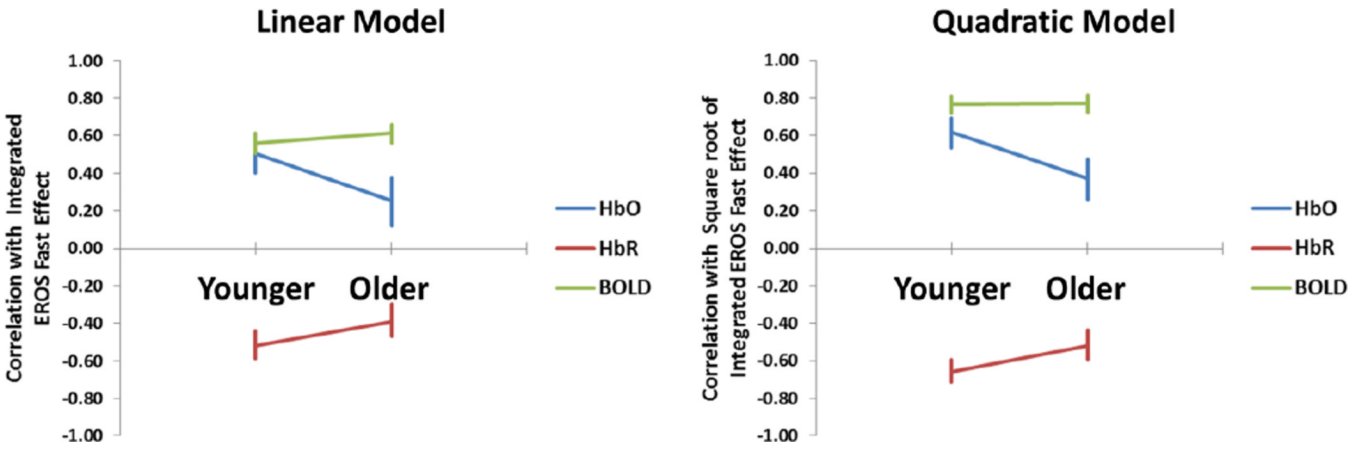

Figure 9.

Average correlations between the observed hemodynamic response and that predicted on the basis of the integration of the fast EROS response over time for younger and older adults. The vertical bars indicate standard errors of the mean computed across subjects.

Table 1

Means (SDs) for the demographic and neuropsychological variables characterizing the subject groups.

Variable	Younger (N=19)	Older High Fit (N=20)	Older Low Fit (N=24)	t test: Y vs. O	t test: OH vs. OL
Number of Females	9	11	13	n.s.	n.s.
Age (years)	22.3 (2.0)	70.3 (4.2)	72.2 (5.2)	$p < .0001$	n.s.
VO2max	-	30.7 (6.7)	18.9 (3.8)	-	$p < .0001$
PASE	-	171.38 (53.42)	121.29 (61.85)	-	$p < .01$
Education (years)	16.5 (1.6)	18.2 (2.5)	15.2 (2.5)	n.s.	$p < .0001$
mMMS	55.7 (1.5)	55.6 (1.2)	54.4 (1.7)	$p < .05$	$p < .01$
WAIS-R Vocabulary	13.5 (1.8)	14.8 (2.8)	12.0 (1.9)	n.s.	$p < .0001$

PASE = Physical Activity Scale for the Elderly

mMMS = modified Mini-Mental Status test

Y vs. O = younger vs. older adults contrast

OH vs. OL = older high-fit vs. older low-fit contrast

Table 2

Means (SDs) for the physiological variables characterizing the subject groups.

Variable	Younger	Older High Fit	Older Low Fit	t test: Y vs. O	t test: OH vs. OL
Height (cm)	-	166.05 (9.20)	166.41 (9.92)	-	n.s.
Weight (kg)	-	68.24 (10.20)	82.24 (19.30)	-	$p < .005$
BMI	-	24.69 (2.59)	29.47 (5.29)	-	$p < .001$
Systolic BP (mm Hg)	114.49 (10.92)	134.98 (16.33)	145.13 (18.24)	$p < .001$	$p < .05$
Diastolic BP (mm Hg)	69.96 (6.24)	71.56 (8.50)	74.83 (11.62)	n.s.	n.s.
Heart Rate (per min)	74.15 (11.15)	65.67 (9.58)	71.64 (12.49)	$p < .10$	$p < .05$

BMI = body mass index

BP = arterial blood pressure

Y vs. O = younger vs. older adults contrast

OH vs. OL = older high fit vs. older low fit contrast